0888-8809/05/$15.00/0
Printed in U.S.A.

Molecular Endocrinology 19(10):2502–2516

doi: 10.1210/me.2004-0397

Trialkyltin Compounds Bind Retinoid X Receptor to Alter Human Placental Endocrine Functions

Tsuyoshi Nakanishi, Jun-ichi Nishikawa, Youhei Hiromori, Hideaki Yokoyama, Mihoko Koyanagi, Shinri Takasuga, Jun-ichi Ishizaki, Mai Watanabe, Shun-ichi Isa, Naoki Utoguchi, Norio Itoh, Yutaka Kohno, Tsutomu Nishihara, and Keiichi Tanaka

Department of Toxicology (T.N., Y.H., H.Y., M.K., S.T., J.I., M.W., S.I., N.I., K.T.) and Laboratory of Environmental Biochemistry (J.N., T.N.), Graduate School of Pharmaceutical Sciences, Osaka University, Suita, Osaka 565-0871; Laboratory of Pharmaceutics (N.U.), School of Pharmaceutical Sciences, Teikyo University, Sagamiko, Kanagawa 199-0195; and Development Division (Y.K.), Fujisawa Pharmaceutical Co., Ltd., Osaka 532-8514, Japan

Retinoid X receptor (RXR) is a nuclear receptor that plays important and multiple roles in mammalian development and homeostasis. We previously reported that, in human choriocarcinoma cells, tributyltin chloride and triphenyltin hydroxide, which are typical environmental contaminants and cause masculinization in female mollusks, are potent stimulators of human chorionic gonadotropin production and aromatase activity, which play key endocrine functions in maintaining pregnancy and fetal development. However, the molecular mechanism through which these compounds stimulate these endocrine functions remains unclear. Our current study shows that trialkyltin compounds, including tributyltin chloride and triphenyltin hydroxide, function as RXR agonists. Trialkyltins directly bind to the ligand-binding domain of RXR with high affinity and function as transcriptional activators. Unlike the natural RXR ligand, 9-*cis*-retinoic acid, the activity of trialkyltins is RXR specific and does not activate the retinoic acid receptor pathway. In addition, trialkyltins activate RXR to stimulate the expression of a luciferase reporter gene containing the human placental promoter I.1 sequence of aromatase, suggesting that trialkyltins stimulate human placental endocrine functions through RXR-dependent signaling pathways. Therefore, our results suggest that activation of RXR may be a novel mechanism by which trialkyltins alter human endocrine functions. (*Molecular Endocrinology* 19: 2502–2516, 2005)

THE RETINOID X receptors RXRα, RXRβ, and RXRγ, which are type II nuclear receptors, are thought to be key factors in several nuclear receptor signaling pathways. These molecules specifically bind 9-*cis*-retinoic acid (9cRA) and thus may be directly involved in the transduction of retinoid signals. In transfected cultured cells, as well as established cell lines, RXRs can act either as homodimers or heterodimeric partners of several other nuclear receptors, including retinoic acid receptors (RARα, -β, and -γ), thyroid hormone receptors (TRα and -β), vitamin D receptor (VDR), peroxisome proliferator-activated receptors (PPARα, -γ, and -δ), and a number of orphan receptors (1–3). Therefore, RXRs may be central to the modulation of several hormonal signals.

The placenta is a transient, but vital, organ for maintaining pregnancy in mammals. Its functions range from nutrient and gaseous exchange to hormone and growth factor production. Several observations suggest that RXRs play indispensable roles in placental development and physiology. In mice, RXRα transcripts are strongly expressed in the ectoplacental cone and, at later stages, in giant trophoblastic cells and the labyrinthine zone of the chorioallantoic placenta (4). RXR knock-out experiments in mice have revealed that RXRα and RXRβ are involved in the formation of the chorioallantoic placenta (5, 6). In particular, the inactivation of RXRα ligand-dependent transcriptional activation function 2, but not ligand-independent transcriptional activation function 1, prevents the formation of labyrinthine trophoblasts and leads to fetal death during the late fetal period or

First Published Online June 7, 2005

Abbreviations: atRA, All *trans*-retinoic acid; CDCA, chenodeoxycholic acid; CG, chorionic gonadotropin; 9cRA, 9 *cis*-retinoic acid; 15dPGJ$_2$, 15-deoxy-$\Delta^{12,14}$-prostaglandin J$_2$; DBTCl$_2$, dibutyltin dichloride; DHA, docosahexaenoic acid; DMSO, dimethyl sulfoxide; DPTCl$_2$, diphenyltin dichloride; DR, direct repeat; FCS, fetal calf serum; FXR, farnesoid X-activated receptor; GST, glutathione *S*-transferase; LBD, ligand-binding domain; LUC, luciferase; MBTCl$_3$, butyltin trichloride; MPTCl$_3$, phenyltin trichloride; PPAR, peroxisome proliferator-activated receptor; RAR, retinoic acid receptor; RXR, retinoid X receptor; RXRE, RXR response element; TBT, tributyltin; TBTBr, tributyltin bromide; TBTCl, tributyltin chloride; TBTH, tribulytin hydride; TBVT, tributylvinyltin; TChTOH, tricyclohexyltin hydroxide; TeBT, tetrabutyltin; TETBr, triethyltin bromide; TMTCl, trimethyltin chloride; TOTH, trioctyltin hydride; TPBS, Tween 20-PBS; TPrTCl, tripropyltin chloride; TPT, triphenyltin; TPTCl, triphenyltin chloride; TPTOH, triphenyltin hydroxide; TR, thyroid hormone receptor; VDR, vitamin D receptor.

***Molecular Endocrinology* is published monthly by The Endocrine Society (http://www.endo-society.org), the foremost professional society serving the endocrine community.**

shortly after birth (7). These placental abnormalities are similar to those found in the placentas of vitamin A-deficient rats (8). These observations suggest that the ligand-dependent transcriptional activation of RXRα is physiologically required for placentation in rodents.

RXRα mRNA and protein have been detected in human cytotrophoblasts and choriocarcinoma cells (9–11). Treatment of these cells with 9cRA and synthetic RXR-specific ligands increases the level of mRNA expression of steroidogenic enzymes, such as aromatase and human (h) chorionic gonadotropin (CG) (9, 10, 12–15). Estrogens and hCG are the principal hormones produced by the placenta during human pregnancy. These hormones are essential for several important events in the establishment and maintenance of pregnancy. Biosynthesis of estrogens requires the catalytic activity of an aromatase enzyme complex, which converts androgenic to estrogenic steroids (16). The human placenta exhibits a high level of aromatase activity and therefore regulates the balance of estrogens *in utero* (17). Altering aromatase function *in utero* can cause permanent effects in human embryos; the lack of placental aromatase causes female pseudohermaphroditism, as is seen in patients with aromatase deficiency (16, 18).

hCG is a luteotropic factor and the primary marker of pregnancy in humans. Stimulation by hCG governs not only progesterone production in the corpus luteum during the first trimester (19) but also testosterone production within the fetal testes (20). Given the pivotal functional roles of aromatase and hCG in sexual development and reproduction, the extant retinoid signals of RXR-mediated transcription in the placenta may greatly alter fetal development because of their disruption of these endocrine functions.

Organotin compounds have been used widely as biocides, agricultural fungicides, wood preservatives, disinfecting agents in circulating industrial cooling waters, and antifouling paints for marine vessels (21, 22). There are many reports of the biological effects of organotin compounds, which vary in their toxic effects to eukaryotes. One of the most notable toxicities in sexual development and reproduction is that of tributyltin (TBT)- and triphenyltin (TPT)-mediated endocrine disruption in some species of gastropods (23, 24). This phenomenon is known as "imposex," the superimposition of male genitalia on female. Therefore, these trialkyltin compounds are suspected to cause endocrine-disrupting effects in mammals, including humans. Human exposure to organotin compounds may result from the consumption of organotin-contaminated meat and fish products, occupational exposure during the manufacture and formulation of organotin compounds, or the application and removal of organotin-containing paints (25, 26). The possible exposure of humans to organotins has therefore aroused great concern about potential toxicities.

Previously, we reported that both tributyltin chloride (TBTCl) and triphenyltin hydroxide (TPTOH) enhance hCG secretion and aromatase activity in human choriocarcinoma cells. In addition, these compounds cause dose-related increases in the steady-state mRNA levels of both hCGβ and aromatase in human choriocarcinoma Jar cells after their exposure to nontoxic concentrations (27). These results suggest that these trialkyltin compounds are potent stimulators of human placental hCG production and aromatase activity *in vitro* and act as endocrine disruptors, the effects of which might alter local hCG and estrogen concentrations in pregnant women. However, the molecular mechanism underlying trialkyltin-induced alterations of human placental endocrine functions remains unclear. To extend our knowledge of the correlation between the structure of organotin compounds and their endocrine-disrupting effects, we assessed the effects of 17 tin compounds on hCG secretion, aromatase activity, and the mRNA levels of hCG and aromatase in Jar cells. We found that the effects of organotin compounds are related to both the number and length of their alkyl chains, suggesting that organotin compounds might interact with a target molecule in a fashion similar to that by which environmental estrogenic chemicals interact with estrogen receptors (28–34). Further, the promoter sequences of both human placental hCGβ and aromatase have several common half-site sequences (T/AGGTCA), of which nuclear receptor response elements typically are composed (13, 14). In addition, expression of both human placental hCG and aromatase is induced by specific RXR ligands (9, 10, 13, 14). In light of all of these results, we hypothesize that organotin compounds interact with RXRs to alter placental endocrine functions. Here we demonstrate that trialkyltin compounds bind to RXRs with high affinity and stimulate transcription through these receptors to alter endocrine functions in human choriocarcinoma cells.

RESULTS

Effects of Organotin Compounds on hCG Production and Aromatase Activity in Human Choriocarcinoma Cells

Previously, we reported that both TBTCl and TPTOH enhance hCG secretion and aromatase activity in human choriocarcinoma cells (27). To extend our knowledge of the correlation between the structures of organotin compounds and their endocrine-disrupting effects, we assessed the effects of 17 tin compounds (Fig. 1) on hCG secretion from, and aromatase activity in, Jar choriocarcinoma cells after their exposure to nontoxic concentrations of these compounds, which were determined from the results of [^{3}H]thymidine uptake assays (data not shown). The most active compounds were TBT or TPT derivatives (Fig. 2, Group III). Exposure to $\geq$ 10 nM of each of these trialkyltin compounds caused statistically significant increases in hCG production by Jar cells. Aromatase activity also

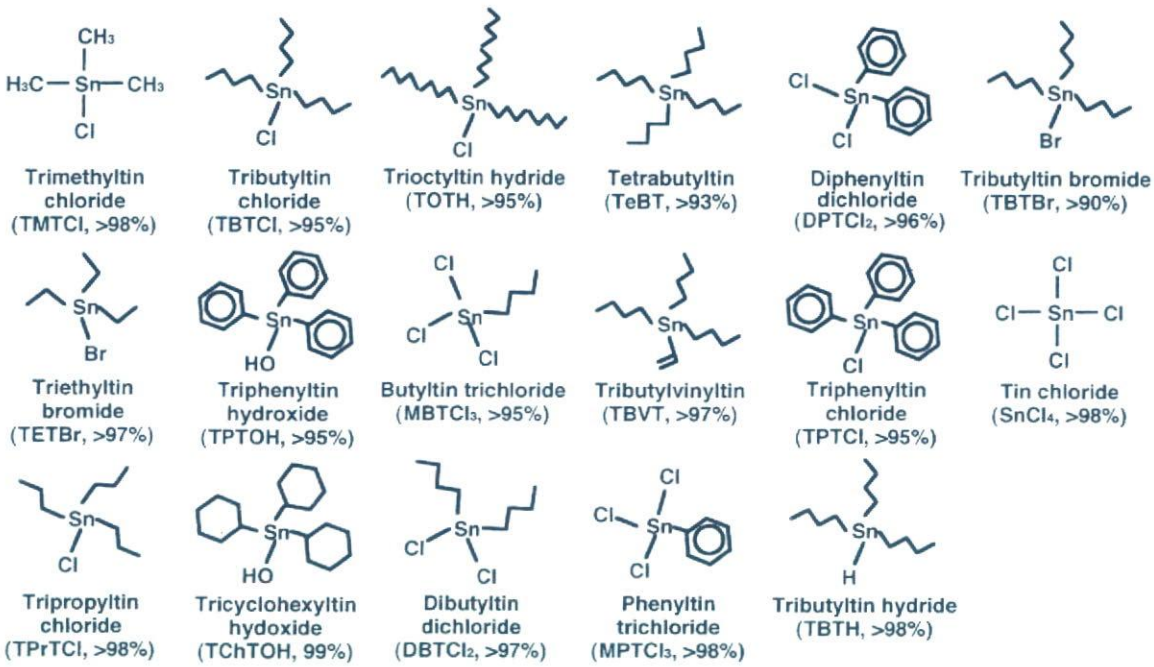

Fig. 1. Structures of the Tin Compounds Used in This Study
The abbreviation for, and purity of, each compound used are indicated in *parentheses*.

increased significantly as the concentrations of the TBT derivatives increased beyond 10 nM or those of the TPT derivatives increased in excess of 30 nM. Among the other trialkyltin compounds (Group I), tripropyltin chloride (TPrTCl) and tricyclohexyltin hydroxide (TChTOH) were active. Like the TBT and TPT compounds, TPrTCl stimulated both hCG production and aromatase activity, whereas TChTOH stimulated hCG production but not aromatase activity. Among the butyltin and phenyltin derivatives (Group II), neither of the mono-alkyltin compounds altered hCG production or aromatase activity. Dibutyltin dichloride ($DBTCl_2$) stimulated aromatase activity at 30 nM but failed to induce hCG production at any of the concentrations tested. In contrast, diphenyltin dichloride ($DPTCl_2$) stimulated hCG production at 30 nM but not aromatase activity at any tested concentration.

There were no significant differences in hCG production and aromatase activity among the TBT and TPT derivatives (Group III), suggesting that the ligand on the trialkyltin (as long as it is not an alkyl group) is relatively unimportant to the stimulation of these endocrine functions. However, the presence of a fourth alkyl group on the tin atom decreased the stimulus potency of the alkyltin compounds on hCG production and aromatase activity, because both tetrabutyltin (TeBT) and tributylvinyltin (TBVT) failed to stimulate these placental functions at doses less than 100 nM (Fig. 2, Group III). These results suggest that the potency of the effects induced by alkyltin compounds is related to both the number and length of the alkyl groups.

In addition, we investigated the tin compound-induced mRNA expression of hCGβ and aromatase at either the concentration that elicited the greatest response in each endocrine function or the maximal nontoxic concentration. The changes in hCGβ and aromatase mRNA expression were almost parallel to those in hCG secretion and aromatase activity (Fig. 3). These results indicate that the observed alkyltin-induced alterations in these placental functions are both caused by regulation at the mRNA level. Such overt correlation between the mRNA expression induced by alkyltin compounds and their structure led us to hypothesize that alkyltin compounds may interact with a nuclear receptor to alter placental endocrine functions; a similar mechanism has been demonstrated for environmental estrogenic chemicals that interact with estrogen receptors (28–34).

Interaction of Alkyltin Compounds with the Hormone-Binding Domain of RXRs

In human placental cells, both hCG production and aromatase activity are controlled by cAMP-dependent intracellular signal pathways. However, in our previous study, neither TBTCl nor TPTOH exerted any effect on cAMP production (27). After a literature search to identify a signaling pathway common to the mRNA expression of both hCG and aromatase, we arrived at the hypothesis that alkyltin compounds act as ligands of RXRs to activate the transcription of hCG and aromatase, because these placental factors are both induced by specific ligands of RXRs (9, 10, 13, 14). In

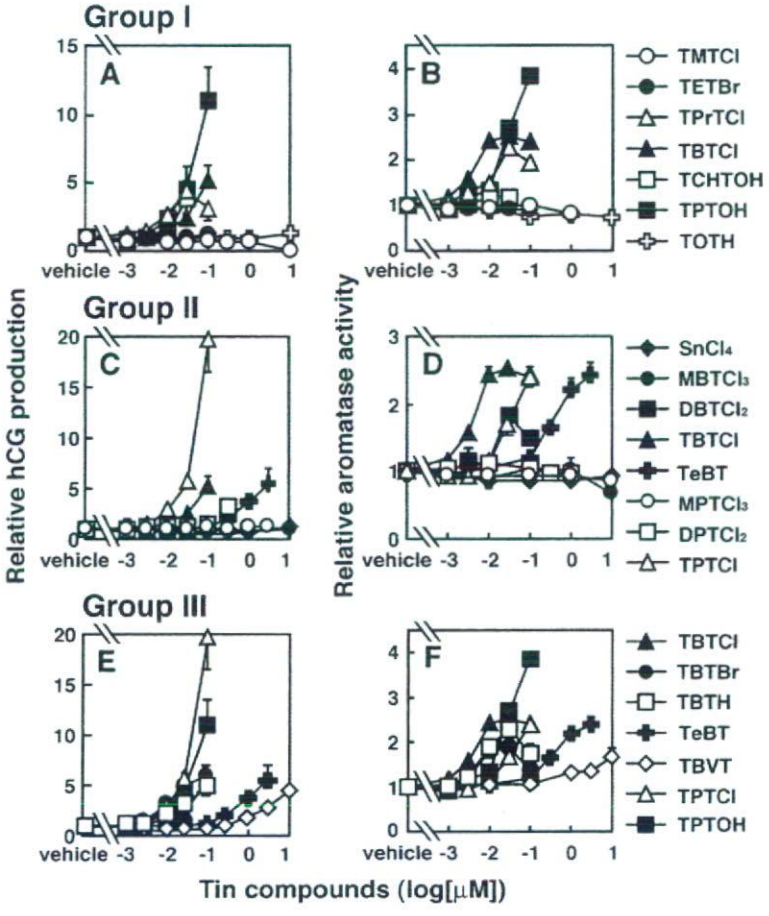

Fig. 2. Effects of Tin Compounds on hCG Secretion (A, C, and E) and Aromatase Activity (B, D, and F) in Jar Cells

Cells were treated with various nontoxic concentrations of tin compounds for 48 h. A nontoxic concentration of a tin compound was defined as a concentration at which the uptake of [^{3}H]thymidine was ≥ 80% that for the vehicle alone (data not shown). Results are expressed as mean ± 1 SD of triplicate cultures. Group I (A and B): comparison of different lengths of alkyl chains in trialkyltin compounds. Group II (C and D): comparison of different numbers of alkyl chains in butyltin and phenyltin compounds. Group III (E and F): comparison of different fourth function groups on the tin of TBT and TPT. The hCG production and aromatase activity in vehicle-only cells, calculated from all experiments, were 290.0 ± 85.3 mIU/well·24 h and 4.08 ± 0.91 pmol/well·4 h, respectively.

fact, we were able to confirm that a natural RXR ligand, 9cRA, and a synthetic RXR-specific ligand, LG100268, induced mRNA expression of both hCGβ and aromatase in Jar cells (Fig. 4).

Accordingly, we examined the dose-response effectiveness of TBTCl and TPTOH in stimulating RXR activity by using human choriocarcinoma JEG-3 cells cotransfected with a human RXRα expression plasmid and a luciferase (LUC) reporter plasmid containing an RXR response element (RXRE). RXR homodimers bind to direct repeat (DR)1 motifs (1–3). We constructed and used pTALDR1, which contains two DR1 sequences, as a reporter plasmid. Treatment with 1–100 nM 9cRA resulted in a 3- to 10-fold increase in LUC activity, whereas similar treatment with LG100268 led to a 3.3- to 4.5-fold increase (Fig. 5A). In addition, 100 nM 9cRA slightly stimulated the expression of LUC in JEG-3 cells transfected with a control plasmid, because JEG-3 cells express endogenous RXRα (10). Treatment of RXRα-transfected JEG-3 cells with 1–100 nM TBTCl stimulated LUC expression 1.5- to 9-fold, and exposing the cells to the same concentrations of TPTOH induced LUC expression 1.8- to 19-fold; these results suggest that low doses of these trialkyltin compounds activate RXR.

To identify the region of RXR involved in activation by alkyltin compounds, we used a chimeric receptor consisting of the DNA-binding domain of the yeast transcription factor GAL4 and the ligand-binding domain (LBD) of RXRα (GAL-RXR). Consistent with the results in Fig. 5A, the activity of the LUC reporter construct in JEG-3 cells cotransfected with the GAL-RXR chimeric receptor and the UAS-LUC reporter increased in a dose-dependent manner after incubation with not only 9cRA but also either TBTCl or TPTOH (Fig. 6). We then investigated the effect of the other tin compounds on activation of GAL-RXR chimeric receptors after exposure of the cells to nontoxic concentra-

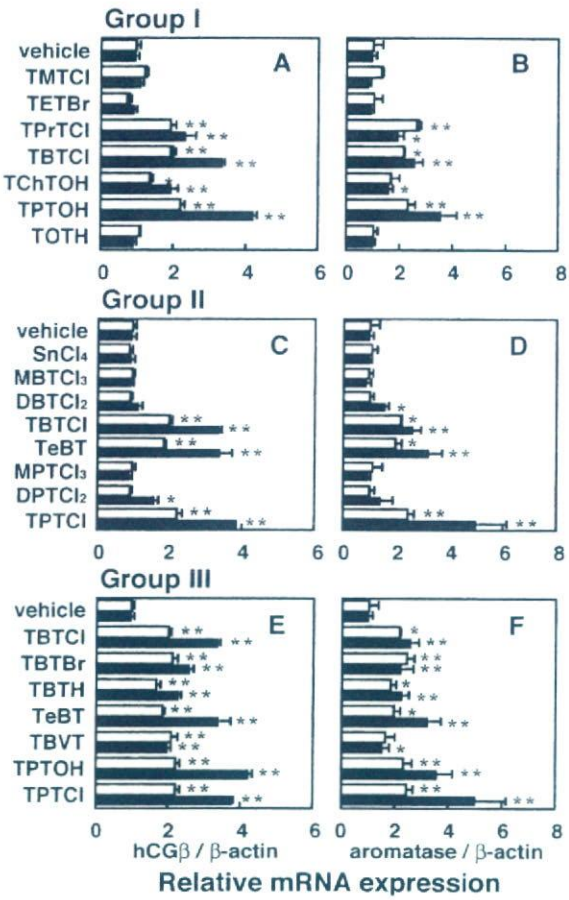

Fig. 3. Effects of Tin Compounds on the mRNA Expression of hCG β (A, C, and E) and Aromatase (B, D, and F) in Jar Cells

Total RNA isolated from Jar cells was treated with tin compounds for 24 h (*open bars*) and 48 h (*solid bars*). The concentrations of each compound were: 10 μM of TOTH, $SnCl_4$, $MBTCl_3$, and TBVT; 3 μM of $MPTCl_3$ and TeBT; 1 μM of 9cRA and TMTCl; 300 nM of $DPTCl_2$; 100 nM of TETBr, TBTCl, TPTOH, TPTCl, TBTBr, and TBTH; and 30 nM of TPrTCl, TChTOH, and $DBTCl_2$. The relative hCGβ and aromatase mRNA levels for each condition were determined by quantitative RT-PCR three times for each of the three independent cultures (see *Materials and Methods*). Results are expressed as mean ± 1 SD of three independent cultures. Groups I (A and B), II (C and D), and III (E and F) correspond to the groups described in the legend for Fig. 2. *, $P < 0.05$; **, $P < 0.01$; and ***, $P < 0.005$ *vs.* vehicle.

tions. TPrTCl, TeBT, and TBVT, as well as the TBT and TPT derivatives, activated transcription through GAL-RXR. TChTOH also activated transcription though GAL-RXR markedly, but the level of activation was only slight compared with that induced by the TBT and TPT derivatives. The level of GAL-RXR activation induced by these tin compounds was almost parallel to the increase in mRNA expression of hCGβ or aromatase in JEG-3 cells treated with these compounds.

RXR serves as a common heterodimerization partner for several receptors (1–3). In addition to RXR

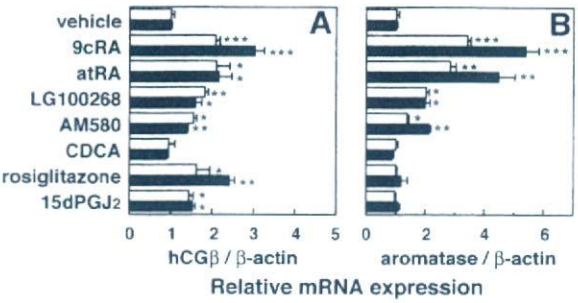

Fig. 4. Effects of Various Nuclear Receptor Agonists on the mRNA Expression of hCG β (A) and Aromatase (B) in Jar Cells

Total RNA isolated from Jar cells was treated with tin compounds for indicated time periods. The concentrations of each compound were: 10 μM of CDCA; 100 nM of 9cRA, atRA, rosiglitazone, or $15dPGJ_2$; and 100 nM of LG100268 or AM580. The relative hCGβ and aromatase mRNA levels for each condition were determined by quantitative RT-PCR three times for each of the three independent cultures (see *Materials and Methods*). Results are expressed as mean ± 1 SD of three independent cultures. *, $P < 0.05$; **, $P < 0.01$; and ***, $P < 0.005$ *vs.* vehicles.

homodimer, RXR-specific ligands can activate two types of complex. One type is the permissive heterodimers, such as PPAR-RXR (35–39) and farnesoid X-activated receptor (FXR)-RXR (40), which can be fully activated by a ligand of either RXR or its partner receptor and are activated synergistically in the presence of both ligands; the other is the conditionally permissive heterodimer RXR-RAR, which can be conditionally activated by RXR ligands only in the presence of an RAR agonist (38, 41). To identify the complexes involved in alkyltin-induced mRNA expression of both placental factors, we assessed the effects of the ligands of various RXR partners. The PPAR ligand 15-deoxy-$\Delta^{12,14}$-prostaglandin J_2 ($15dPGJ_2$) and the PPARγ-specific ligand rosiglitazone induced mRNA expression of hCGβ, but not aromatase, in Jar cells. Chenodeoxycholic acid (CDCA), an FXR agonist, failed to increase the mRNA expression of either placental factor. However, a natural RAR ligand, all-*trans*-retinoic acid (atRA), and a synthetic RARα-specific ligand, AM580, induced expression of the mRNA of both hCGβ and aromatase in human placental cells, as previously described (15). Furthermore, the natural RXR ligand 9cRA also can function as an RAR agonist to transactivate RXR-RAR heterodimer (1–3, 42). Accordingly, we examined whether typical trialkyltin compounds, which function as RXR agonists, can activate RXR-RAR transcription, as does 9cRA, by using LUC reporter plasmids containing an RAR response element (DR2 or DR5). Cells simultaneously transfected with human RXRα and RARβ expression vectors dramatically respond to atRA and 9cRA (Fig. 5B). Although TBTCl and TPTOH also stimulated the expression of LUC, the effectiveness of these organotin compounds was comparable to

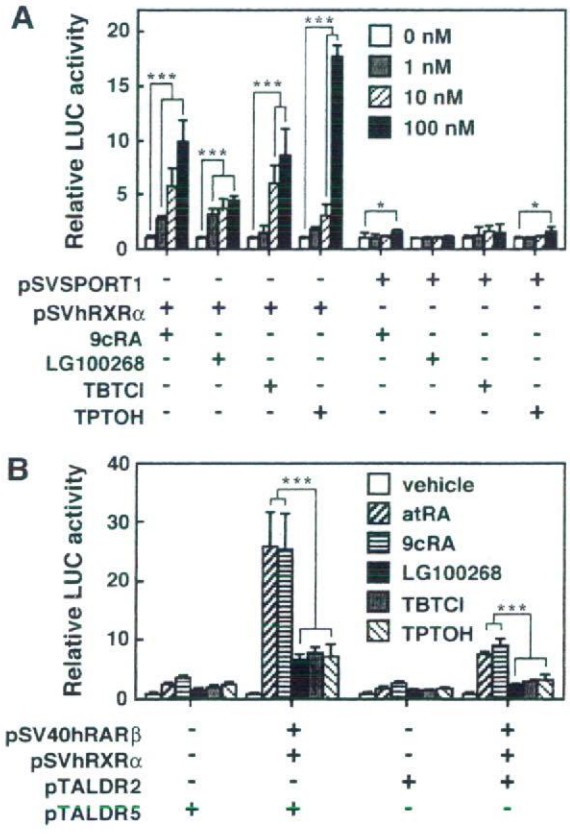

Fig. 5. Ability of TBTCl and TPTOH to Activate RXR and RAR

A, JEG-3 cells were cotransfected with 10 ng of either pSVhRXRα or pSVSPORT1 in addition to 0.1 μg pTALDR1 (see *Materials and Methods*) and then treated with various concentrations of 9cRA, LG100268, TBTCl, or TPTOH. B, JEG-3 cells were cotransfected with 10 ng each of pSVhRXRα and pSV40hRARβ in addition to 50 ng pTALDR2 or pTALDR5 and then treated with 100 nM of atRA, 9cRA, LG100268, TBTCl, or TPTOH. pRL-TK (2 ng) was cotransfected as the control for normalization (see *Materials and Methods*). The results are expressed as average fold activation ± 1 SD after normalization to *Renilla* LUC activity. *, $P < 0.05$; **, $P < 0.01$; and ***, $P < 0.005$.

that of LG100268, which does not transactivate RXR-RAR heterodimer (Fig. 5B). In addition, we examined the effect of TBTCl and TPTOH on activation of RARα, -β, and -γ by using chimeric receptors in which the GAL4 DNA binding domain was fused to the LBD of RARs (GAL-RARs) instead of RXRα. Neither alkyltin compound activated transcription through GAL-RARs (data not shown). These results suggest that the alkyltin compounds, which activate transcription of the reporter construct through GAL-RXR, interact with the LBD of RXR and transactivate RXR homodimer, but not RXR-RAR heterodimer, unlike 9cRA. Taken together, these results suggest that RXR homodimer may be involved in the alkyltin-induced mRNA expression of both placental factors, provided that the hCGβ induced also involves PPAR-RXR heterodimers.

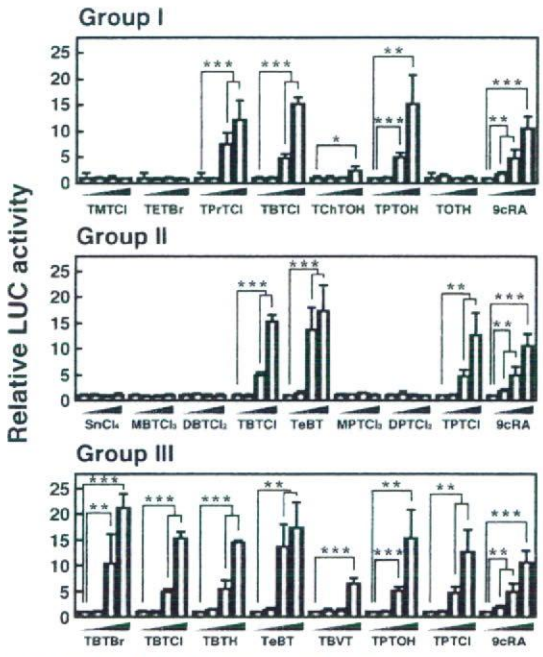

Fig. 6. Ability of Tin Compounds to Activate GAL-RXR

JEG-3 cells were cotransfected with 10 ng p4xUAS-tk-luc, 5 ng pBK-CMV-GAL4-hRXRα, and then treated with 9cRA or each of the tin compounds. The doses of each compound were: 0, 1, 10, or 100 nM of 9cRA, TETBr, TBTCl, TPTOH, TPTCl, TBTH, or TBTBr; 0, 0.1, 1, or 10 μM of TOTH, $SnCl_4$, $MBTCl_3$, or TBVT; 0, 1, 10, or 30 nM of TPrTCl, TChTOH, or $DBTCl_2$; 0, 0.1, 1, or 3 μM of $MPTCl_3$ or TeBT; 0, 10, 100, or 300 nM of $DPTCl_2$; and 0, 10, 100, or 1000 nM of TMTCl. pRL-TK (2 ng) was cotransfected as the control for normalization (see *Materials and Methods*). The results are expressed as average fold activation ± 1 SD after normalization to *Renilla* LUC activity. Groups I, II, and III correspond to the groups described in Fig. 2. *, $P < 0.05$; **, $P < 0.01$; and ***, $P < 0.005$.

Binding of Tin Compounds to RXR

To characterize the binding affinities of these tin compounds to RXR directly, we performed analyses of the saturation binding of [^{14}C]TPTOH and [^{3}H]9cRA to chimeric receptors, which consisted of glutathione *S*-transferase (GST) fused to the LBD of human RXRs (GST-RXRs). The binding of 9cRA to GST-RXRs was specific and saturative (Fig. 7). Scatchard analyses of the binding of [^{3}H]9cRA to GST-RXRα, -β, and -γ yielded dissociation constant (K_d) values of 11.7, 15.5, and 8.66 nM, respectively. These K_d values were similar to those previously reported (3, 42), suggesting that this system is useful for determining the binding affinity of alkyltin compounds to RXRs. Scatchard analyses of the binding of [^{14}C]TPTOH to RXRα, -β, and -γ yielded K_d values of 55.5, 241, and 95.3 nM, respectively (Fig. 7). Although the K_d values of TPTOH for RXRs were approximately 5- to 15-fold higher than those for 9cRA, our results indicate that TPTOH binds to the RXRs with high affinity in a saturable and specific manner.

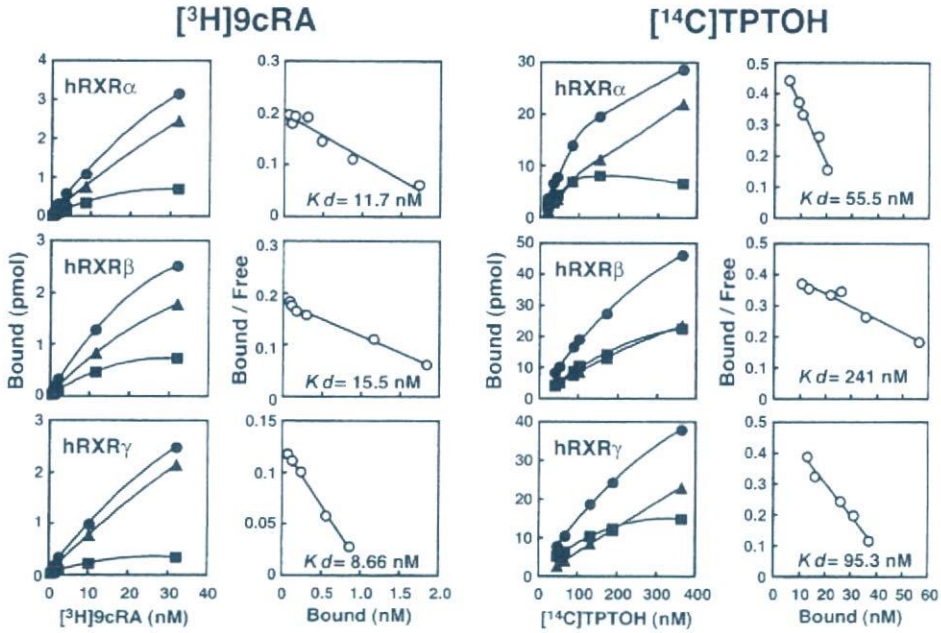

Fig. 7. Saturation Kinetics for the Binding of [^{3}H]9cRA and [^{14}C]TPTOH to hRXRα, -β, and -γ

Specific binding (*solid square*) is defined as total binding (*solid circle*) minus nonspecific binding (*solid triangle*). Scatchard analysis was performed on specific binding data (triplicates at each point) to yield the indicated dissociation constants (K_d value) for each receptor.

To further test which of the other tin compounds might bind to RXR as a ligand, we performed competitive ligand-binding assays. We measured the ability of [^{3}H]9cRA or [^{14}C]TPTOH to compete with the tin compounds for binding to GST-RXRα. The TBT and TPT derivatives all competed with [^{3}H]9cRA for binding to GST-RXRα in a concentration-dependent manner (Fig. 8). Consistent with the K_d value of TPTOH for RXRα, the IC_{50} value of TPTOH for binding [^{3}H]9cRA was approximately 5-fold higher than that of unlabeled 9cRA. The IC_{50} values of the other TBT and TPT derivatives for binding [^{3}H]9cRA were almost the same as that of TPTOH, demonstrating that these trialkyltin compounds bind directly to RXR. In contrast to the results of competitive assay for [^{3}H]9cRA, 9cRA failed to completely out compete [^{14}C]TPTOH for binding to GST-RXRα, whereas the TBT and TPT derivatives successfully competed for binding (Fig. 8B). The IC_{50} value of 9cRA for binding [^{14}C]TPTOH was more than 10-fold higher than those of TBTs and TPTs (Table 1). Further, TPrTCl bound to GST-RXRα as well as did the TBT and TPT derivatives, because its IC_{50} values for binding [^{3}H]9cRA and [^{14}C]TPTOH were almost the same as those of the TBT and TPT derivatives (Fig. 8 and Table 1). However, TChTOH, TeBT, and TBVT failed to compete with [^{3}H]9cRA for binding to GST-RXRα, despite their ability to activate RXRα. Although TChTOH out competed [^{14}C]TPTOH for binding to GST-RXRα, TeBT only slightly out competed [^{14}C]TPTOH, and TBVT failed to compete with [^{14}C]TPTOH for binding to GST-RXRα (Table 1). By contrast, triethyltin bromide (TETBr), which was unable to activate transcription through an RXR, bound weakly to GST-RXRα. The IC_{50} values of TETBr for binding [^{3}H]9cRA and [^{14}C]TPTOH were approximately 25- to 50-fold higher than those of the TBT and TPT derivatives (Table 1). The remaining tin compounds (trimethyltin chloride, TMTCl; trioctyltin hydride, TOTH; butyltin trichloride, $MBTCl_3$; phenyltin trichloride, $MPTCl_3$; $DBTCl_2$; $DPTCl_2$; and $SnCl_4$) did not compete successfully with either [^{3}H]9cRA or [^{14}C]TPTOH for binding to GST-RXRα, suggesting that they were unable to bind to RXRs.

Trialkyltin Compounds Stimulate the Expression of an LUC Construct Containing the Human Placental I.1 Sequence of Aromatase via Activation of RXRα

To determine whether trialkyltin compounds, which bind to and activate RXRs, induce aromatase expression in the human placenta via ligand-dependent activation of RXRs, we assessed the dose-response effectiveness of TBTCl and TPTOH by using JEG-3 cells cotransfected with a human RXRα expression plasmid and a LUC reporter plasmid containing the promoter sequence (−2295 to +107 bp) of exon I.1, which is the major promoter of human placental aromatase (Fig. 9A; and Refs. 16, 43, and 44). As expected, LG100268 stimulated the expression of LUC by 2.4- to 3.5-fold. These results suggest that the aromatase promoter is regulated by ligand-bound RXR (13). In addition, TBTCl and TPTOH stimulated the expression of LUC in

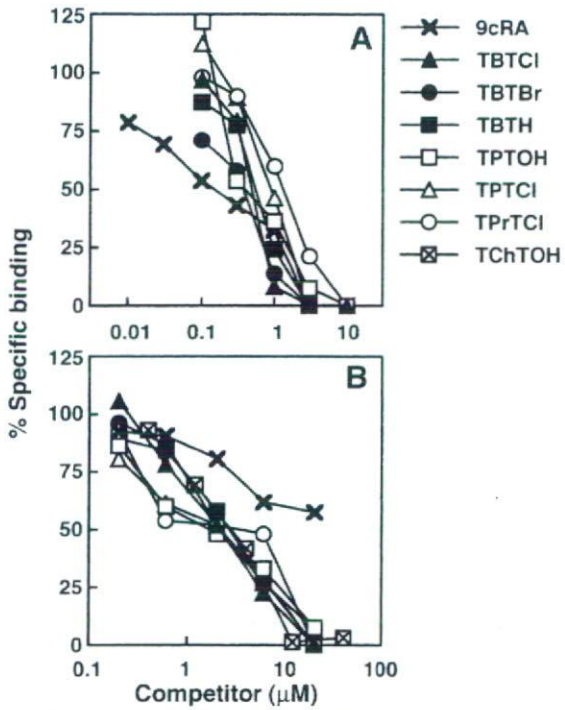

Fig. 8. Competition by 9cRA and Alkyltin Compounds with [^{3}H]9cRA (A) and [^{14}C]TPTOH (B) for Binding to the LBD of hRXRα

The LBD of hRXRα protein was incubated with increasing concentrations of unlabeled 9cRA or alkyltin compounds as competitors in the presence of [^{3}H]9cRA or [^{14}C]TPTOH as ligand. Results are expressed as percent specific binding. Each experiment was performed at least twice, and representative curves are shown.

a dose-dependent manner to levels approaching those induced by 9cRA and LG100268.

Because RAR agonists induced mRNA expression of aromatase (Fig. 4B), we examined the effectiveness of cotransfection with a human RARβ expression plasmid in stimulating the LUC activity by these alkyltin compounds to identify whether RAR is involved in alkyltin-induced aromatase expression (Fig. 9B). In the presence of the natural RAR ligands, atRA or 9cRA, RAR statistically significantly increased the expression of LUC ($P < 0.05$ or $P < 0.01$), whereas RAR had no effect on the LUC activity induced by LG100268, TBTCl, or TPTOH (Fig. 9B). These results suggest that the expression of human placental aromatase induced by these alkyltin compounds is involved in a ligand-dependent signaling pathway of RXRs but not in transactivation of RXR-RAR.

DISCUSSION

Although our previous study of human placental cells showed that TBTCl and TPTOH enhance hCG secretion and aromatase activity with an accompanying increase in the mRNA expression of each factor (27),

Table 1. IC_{50} of Tin Compounds for Competition of [^{3}H]9cRA and [^{14}C]TPTOH Binding to hRXRα, and EC_{50} of Tin Compounds for GAL-RXR Reporter Assay

Compound	IC_{50} of Competition Assay (μM)		EC_{50} of GAL-RXR Activity (nM)
	[^{3}H]9cRA	[^{14}C]TPTOH	
9cRA	0.107	26.9	10.2
TBTCl	0.468	2.26	14.4
TBTH	0.475	2.37	12.3
TBTBr	0.265	2.56	10.4
TPTOH	0.527	1.82	13.9
TPTCl	0.792	1.63	13.4
TPrTCl	0.921	2.11	9.0
TChTOH	>10	2.68	17.3
TeBT	>10	23.7	559
TBVT	>10	>200	2960
TETBr	6.76	80.1	N.D.[a]
TMTCl	>10	>200	N.D.
TOTH	>10	>200	N.D.
$SnCl_4$	>10	>200	N.D.
$MBTCl_3$	>10	>200	N.D.
$DBTCl_2$	>10	>200	N.D.
$MPTCl_3$	>10	>200	N.D.
$DPTCl_2$	>10	>200	N.D.

[a] Not detectable.

the underlying molecular mechanism had remained unclear. In our previous study, we examined the effect of TBTCl and TPTOH on cAMP concentrations in human choriocarcinoma cells, because hCG production and aromatase activity in the human placenta are both well known to be controlled by cAMP-dependent intracellular signal pathways (16, 17, 45, 46). However, neither of these trialkyltin compounds altered cAMP production (27). We then speculated that activation of RXRs is a common signaling pathway of alkyltin-stimulated hCG production and aromatase activity, because both of these events are induced by specific ligands of RXRs (Fig. 4 and Refs. 9, 10, 13, and 14). In our present study, we provide evidence that trialkyltin compounds stimulate the transcription of RXRs because of a high-affinity interaction with the LBD of the receptor. In addition, trialkyltin compounds stimulate the expression of an LUC reporter construct containing the human placental promoter I.1 sequence of aromatase via a ligand-dependent signaling pathway of RXR.

In humans, the tissue-specific expression of aromatase is strictly regulated. Human aromatase is a single-copy gene composed of 10 exons: exons II through X encode the aromatase protein as well as the 3′-untranslated region of mRNA common to all estrogen-producing tissues (16). There are a number of variants of exon I. These encode the 5′-untranslated regions of various aromatase mRNAs, which are selectively expressed in some tissues by alternative splicing (16, 43, 44). The tissue-specific expression of aromatase in humans appears to be mediated by tis-

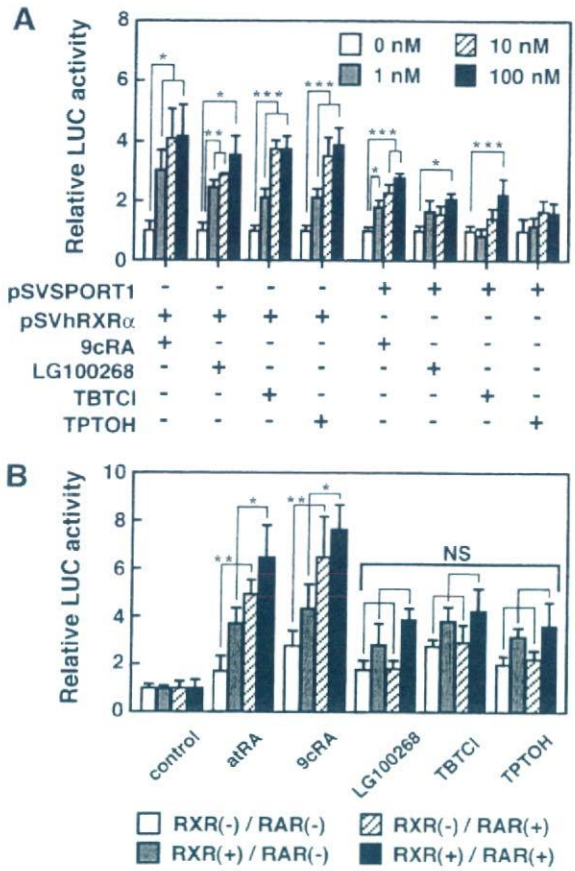

Fig. 9. Ability of TBTCl and TPTOH to Increase Transcription of an LUC Reporter Gene Containing the Human Placental Promoter I.1 Sequence of Aromatase via the Activation of RXR but not RAR

A, JEG-3 cells were cotransfected with 10 ng of either pSVhRXRα or pSVSPORT1 in addition to 50 ng PGVArom and then treated with various concentrations of 9cRA, LG100268, TBTCl, or TPTOH. B, JEG-3 cells were cotransfected with 10 ng pSVhRXRα or pSV40hRARβ, or both, in addition to 50 ng PGVArom, and then treated with 100 nM of atRA, 9cRA, LG100268, TBTCl, or TPTOH. pRL-TK (2 ng) was cotransfected as the control for normalization (see *Materials and Methods*). The results were expressed as average fold activation ± 1 SD after normalization to *Renilla* LUC activity. *, $P < 0.05$; **, $P < 0.01$; and ***, $P < 0.005$. NS, Not significant ($P \geq 0.05$).

sue-specific promoters lying upstream of the respective exon I sequences and by the binding of transcription factors to specific regions of each promoter. In the placenta, aromatase is driven by the placental major promoter (I.1), and the transcript contains exon I.1. In contrast to our results, Saitoh *et al.* (47) recently reported that TBT inhibits aromatase activity and decreases mRNA levels in ovarian granulosa cells. They also suggested that TBT-induced suppression of aromatase in the cells is partly regulated at the transcriptional level because of association with the cAMP-protein kinase A pathway or regulation by the steroidogenic tissue-specific transcriptional factor adrenal 4 binding protein/steroidogenic factor 1. In contrast to those in the placenta, ovarian transcripts of aromatase contain a 5′ sequence immediately upstream of the translation start site, because expression of the gene in the ovary uses a proximal promoter (II) that is strongly regulated by adrenal 4 binding protein/steroidogenic factor 1 and cAMP. In addition, RXR and PPARγ ligands suppress the mRNA expression of aromatase in ovarian granulosa cells (48, 49). Therefore, in light of our findings, TBT-induced suppression of aromatase in ovarian granulosa cells may involve RXR activation.

The RXRs stand out as unique members of the type II nuclear receptor subfamily and play a dual role in nuclear receptor signaling. On one hand, they can bind to their own response element (DR1) as a homodimer and activate transcription in response to their ligands, and, on the other hand, they serve as partners for other nuclear receptors (1–3). Trialkyltin compounds bind to RXRs to induce their transcription. In turn, the expression of hCG and aromatase induced by these compounds may involve either RXR-homodimer or -heterodimer, or both. The existence of three types of heterodimers—nonpermissive, conditionally permissive, and fully permissive—has been described. Nonpermissive heterodimers include RXR-TR and RXR-VDR, which cannot be activated by RXR agonist regardless of the presence (or absence) of the agonist of its partner receptor; formation of the heterodimer is thought to preclude the binding of ligand to RXR (50, 51). RXR-ligand-dependent transcription in promoter I.1 of human aromatase is reported to be regulated by RXR-VDR heterodimers, owing to binding to the imperfect palindromic sequence located from −183 to −172 bp upstream of the transcriptional start site (13). However, within these complexes, RXR acts as a silent partner, as described earlier (50). In addition, we used a GAL-VDR chimeric receptor to confirm that TBT and TPT could not activate transcription of VDR (data not shown). Consequently, both alkyltin-induced aromatase activity and mRNA expression may not involve the association of RXR-VDR. Although RXR-TR heterodimer generally is believed to be nonpermissive (51), Castillo *et al.* (52) recently demonstrated that RXR-TR heterodimer can function as a permissive heterodimer to allow 9cRA-induced stimulation of prolactin gene transcription in rat pituitary cells. Accordingly, we used a synthetic DR4 reporter gene to examine whether TBTCl and TPTOH stimulate transcription of RXR-TR heterodimer. However, these trialkyltin compounds had no effect on transactivation of these complexes in the presence or absence of T_3. We then used a GAL-TR chimeric receptor to confirm that TBT and TPT could not activate transcription of TR (data not shown). These results suggest that these trialkyltin-induced transcriptional activities also do not involve the association of RXR-TR.

As an example of the second type of heterodimer, the RXR-RAR heterodimer exhibits conditional permissivity because full response to RXR agonist occurs only in the presence of an RAR agonist (38, 41). Our

results showed TBT and TPT function as RXR agonists but not RAR agonist. Although RXR-RAR heterodimer generally is believed to be nonpermissive in the absence of RAR agonist, LG100754, which binds to RXRs but not RARs, strongly transactivates this heterodimer pair (53). In addition, the mRNA expression of both hCG and aromatase is also induced by RAR-specific agonist (Fig. 4), and it is possible that in light of the result in Fig. 9B, the transcription from promoter I.1 of human aromatase may be regulated by RXR-RAR heterodimers. However, TBTCl and TPTOH failed to transactivate RXR-RAR heterodimer on either RAR response element (DR2 and DR5) reporter elements or promoter I.1 elements of human aromatase (Figs. 5B and 9B). These results suggest that, unlike the effect of LG100754, these trialkyltin-induced transcriptional activities do not involve the association of RXR-RAR.

The third type is the permissive heterodimers, such as PPAR-RXR and FXR-RXR, which exhibit dual ligand permissivity, because they can be activated by the agonists of either RXR or its partner receptor, or both, in a more-than-additive fashion (35–40). The PPAR ligand $15dPGJ_2$, PPARγ-specific ligand rosiglitazone, and FXR ligand CDCA all failed to increase mRNA expression of aromatase in Jar cells (Fig. 4B), suggesting that neither PPAR-RXR nor FXR-RXR heterodimers are involved in organotin-induced aromatase expression in the human placenta and that RXR homodimer may be required for organotin-induced aromatase expression. By contrast, PPAR agonists, in addition to RXR and RAR agonists, stimulate mRNA expression of hCGβ, as previously described (Fig. 4 and Refs. 9, 10, 12, and 14). These findings indicate that organotin-induced hCGβ expression might involve either PPAR-RXR heterodimers or RXR homodimer.

To address these possibilities, we constructed a LUC reporter plasmid containing the promoter sequence (−455 to +365 bp) of hCGβ5, which is the predominant hCGβ subunit expressed in the human placenta, and assessed the effectiveness of TBTCl and TPTOH in stimulating LUC activity by using JEG-3 cells cotransfected with a human RXRα expression plasmid and the hCGβ5-LUC reporter plasmid. However, trialkyltin compounds, RXR, and PPAR ligands failed to stimulate LUC expression (data not shown), whereas cAMP analogs stimulated gene expression, as previously described (45). Furthermore, Tarrade *et al.* (14) reported that ligand-dependent mRNA expression of hCGβ is transcriptionally controlled by PPARγ-RXR heterodimers, which bind to DR1 as well as does RXR homodimer. However, like us, they failed to detect expression of reporter gene constructs containing imperfect DR1 motifs in the regulatory region of the hCGβ gene. Transcriptional regulation in promoter I.1 of human aromatase and the hCGβ promoter is not yet fully understood, and neither the PPAR response element nor the RXRE involved in both promoter activation by RXR ligands has been identified. Further studies are needed to clarify the precise mechanism of action of RXRs in the expression of human placental aromatase and hCG, because the ligand-dependent signaling pathways of RXRs appear intricate.

We assayed 15 tin compounds, in addition to TBTCl and TPTOH, for their ability not only to induce hCG production, aromatase activity, and mRNA expression of both factors but also to activate RXR through binding to the LBD of the receptor. hCG production and aromatase activity did not differ significantly among the TBT and TPT derivatives. In addition, the abilities to bind to the LBD of RXR and activate the receptor were similar among these compounds, because they all competed with both [^{3}H]9cRA and [^{14}C]TPTOH for binding to RXR approximately as well as did TBTCl and TPTOH. These results suggest that the exact identity of the ligand on the trialkyltin (as long as it is not another alkyl group) is relatively unimportant for binding to RXR.

By contrast, approximately 50- to 100-fold higher concentrations of tetraalkyltin compounds such as TeBT and TBVT were needed to elicit a response, compared with those of the TBT and TPT derivatives. In addition, although the tetraalkyltin compounds stimulated transcription through RXR, they hardly competed with [^{3}H]9cRA for binding to the LBD of RXR. This observation may indicate that the tetraalkyltin compounds were metabolically converted to the active form in the cells. This hypothesis is supported by the general trend of the previous results showing that organotin compounds undergo dealkylation by the microsomal monooxygenase system, which is dependent on cytochrome P450 in the liver and other organs (54–56). The presence of a fourth alkyl group on the tin atom may interfere with the binding of alkyltin compounds to RXR, and activation of the receptor by these tetraalkyltin compounds may be the result of their metabolic conversion in cells to the active dealkylated form (*e.g.* TBT). Such events are reminiscent of an early observation that atRA could activate RXR in cells because of its metabolic conversion to the high-affinity ligand 9cRA (57). Although the dialkyltin compounds neither bind to nor activate RXR, $DBTCl_2$ and $DPTCl_2$ induced expression of the mRNA of aromatase and hCGβ, respectively. It remains unclear why these dialkyltin compounds induced expression of the mRNA of aromatase or hCGβ, but the induction appears to be caused by a mechanism other than activation of RXRs.

Among the trialkyltin compounds other than TBT and TPT derivatives, TPrTCl was most active. TPrTCl activated transcription of RXR as well as did 9cRA and, like TBTCl and TPTOH, completely out competed both [^{3}H]9cRA and [^{14}C]TPTOH for binding to RXR. TETBr bound weakly to RXR, but we were unable to detect TETBr-induced transcription of RXR and mRNA expression of hCGβ and aromatase. The fact that TETBr is cytotoxic at concentrations greater than 300 nM, according to the result of the [^{3}H]thymidine uptake assay (data not shown), may render TETBr-stimulated RXR activation undetectable. TChTOH, which activated transcription of RXR, completely out competes [^{14}C]TPTOH for binding to the LBD of RXR, whereas it

cannot out compete [^{3}H]9cRA at all. This difference in the ability of TChTOH to compete with [^{3}H]9cRA and [^{14}C]TPTOH may be caused by differences in their ligand-protein contacts (see following paragraph). These results suggest that the affinity of tin compounds to RXR is related to both the numbers and lengths of their alkyl groups.

RXR has been characterized as a nuclear receptor that demonstrates a highly restricted substrate specificity. Until recently, 9cRA was defined as the most potent RXR activator. However, various fatty acids, such as docosahexaenoic acid (DHA) and phytanic acid, and methoprene acid, a synthetic juvenile hormone analog used as an insect regulator, have been identified as RXR ligands (58–62). In addition, several retinoids with RXR selectivity have been developed (63), because retinoids are important therapeutic agents in the treatment of cancer and proliferative diseases of the skin. Although fatty acid- or methoprene acid-induced RXR activation requires greater than 1000-fold higher concentrations than that induced by 9cRA (58–62), the protein-ligand interactions of almost all RXR ligands share several common characteristics. Recently, Egea *et al.* (64) have obtained some interesting findings through analyzing the crystal structures of RXR with DHA, the synthetic ligand BMS649, and 9cRA. For example, RXR ligands contain a carboxylate group, which is important in their ability to be buried stably in the predominantly hydrophobic pocket. This functional group is involved in an ionic interaction with the strictly conserved basic residue R316 of helix H5 and forms a hydrogen bond with the backbone carbonyl amide group of the β-turn residue A327. Furthermore, ligand atoms C14–C22 of DHA and the tetrahydrotetramethylnaptho group of BMS649 occupy the same hydrophobic cavity (delineated by helices H3, H7, and H11), in which the β-ionone ring of 9cRA is buried stably. However, although trialkyltin compounds bind RXR with high specificity and induce RXR activation at doses similar to those of 9cRA, they lack a carboxylate group. Further, except for the TPT derivatives and TChTOH, RXR-stimulating trialkyltin compounds also lack sufficiently long fatty acid and cyclic functional groups, both of which might be buried in the β-ionone binding subpocket. In the competitive ligand-binding assay, RXR-stimulating trialkyltin compounds, except for TChTOH, completely out competed both [^{3}H]9cRA and [^{14}C]TPTOH, whereas 9cRA could not completely out-compete [^{14}C]TPTOH for binding to RXR. In addition, TChTOH out competed [^{14}C]TPTOH but not [^{3}H]9cRA. Together, these results suggest that the protein-ligand interaction of trialkyltin compounds and RXR is very different from those seen with other RXR ligands. Indeed, previous studies have reported that, despite the overall similarity of protein-ligand interactions, RXR ligands differ, especially within the L-shaped binding pocket. Although further studies are necessary to clarify which amino acid of RXR is important to the binding of trialkyltin compounds to the ligand-binding pocket, the ligand-protein contacts of these trialkyltin compounds are probably unique to them.

To our knowledge, ours is the first study to clarify the molecular mechanism of trialkyltin-induced endocrine-disrupting effects in the human placenta. Through RXR activation, trialkyltin compounds may be potent endocrine disruptors of other human tissues, because these compounds alter the endocrine functions, differentiation, and other processes of several human cell types (21, 47, 65–67). Furthermore, we demonstrated that trialkyltin compounds function as RXR ligands with novel structures, which bind to the LBD of RXR with high affinity and stimulate transcription of the receptor. We believe that our results provide information useful in the design of novel RXR ligands.

MATERIALS AND METHODS

Chemicals and Cell Culture

TBTCl, TPTOH, TOTH, and $DBTCl_2$ were obtained from Tokyo Kasei Kougyo (Tokyo, Japan). $SnCl_4$, TMTCl, TETBr, TChTOH, $MBTCl_3$, $MPTCl_3$, $DPTCl_2$, TPTCl, TBTH, TBTBr, TeBT, and TBVT were obtained from Aldrich Chemicals (Milwaukee, WI). 9cRA, atRA, AM580, and CDCA were obtained from Sigma Chemical Co. (St. Louis, MO). 15dPGJ_2 and rosiglitazone were obtained from Cayman Chemical (Ann Arbor, MI). TPrTCl was obtained from Merck (Darmstadt, Germany). LG100268 (>95% pure) was synthesized in the Medical Chemistry Laboratories of Fujisawa Pharmaceutical (Osaka, Japan). Human choriocarcinoma cell lines Jar and JEG-3 were obtained from American Type Culture Collection (ATCC; Manassas, VA). Jar cells (ATCC No. HTB-144) were cultured in RPMI 1640 medium with 2 mM L-glutamine, 1 mM pyruvate, 4.5 g/liter glucose, and 10% fetal calf serum (FCS). JEG-3 cells (ATCC no. HTB-36) were cultured in MEM with 2 mM L-glutamine, 0.1 mM MEM nonessential amino acid solution (Invitrogen, Carlsbad, CA), and 10% FCS. To determine the effect of tin compounds on hCG secretion, aromatase activity, and mRNA expression of Jar cells, the cells were seeded and precultured for 24 h and then treated with either various concentrations of tin compounds in 0.1% dimethyl sulfoxide (DMSO) or vehicle alone (0.1% DMSO) for an additional 24 or 48 h. In control experiments, 0.1% DMSO did not alter hCG secretion, aromatase activity, mRNA expression of hCGβ and aromatase, or the results of reporter gene assays in any of the cell lines examined.

Determination of hCG Production in Culture Media

hCG production was assessed as previously described (27). Jar cells were seeded in 48-well plates (4×10^4 cells per well) in regular culture medium supplemented with 5% charcoal-stripped FCS instead of 10% normal FCS. After 24 h, cells were treated with various tin compounds for 48 h. To determine hCG production, the cells were then washed and cultured in fresh medium for another 24 h. Culture supernatant was collected, and hCG concentration was determined by ELISA. Microtiter ELISA plates were coated with 5 μg/ml rabbit polyclonal antibody against intact hCG in 0.05 M sodium bicarbonate, 0.02 M sodium carbonate buffer (pH 9.6) overnight at 4 C. They were blocked for 2 h at room temperature with 1% (wt/vol) gelatin in PBS, washed with 0.05% (vol/vol) Tween 20 in PBS (TPBS), and incubated for 2 h at 37 C with 50 μl collected test samples. After being washed three times with TPBS, the plates then were incubated for 2 h at 37

C with 1:1000 mouse monoclonal antibody against the β-subunit of hCG. After being washed with TPBS, the plates were incubated for an additional 2 h at 37 C with 1:1000 rabbit antimouse IgG1 antibody conjugated with horseradish peroxidase (Zymed Laboratories, Inc., South San Francisco, CA). The plates then were washed with TPBS and developed using 2.5 mM 2,2′-azinobis(3-ethylbenzothiazoline-6-sulfonic acid) diammonium salt (Sigma) in 0.1 M citrate buffered solution containing 0.015% H_2O_2. The reaction was stopped by the addition of 0.1% NaN_3, after which the plates were read at a wavelength of 415 nm in a microplate reader (Bio-Rad Laboratories, Inc., Hercules, CA). The level of hCG in the culture supernatant was calculated from a standard curve by using Microplate Manager III software (Bio-Rad). The standardized hCG was a kind gift from Teikoku Hormone Manufacturing (Tokyo, Japan).

Aromatase Assay

Aromatase activity was determined as previously described (27). Jar cells were seeded in 12-well plates (1.5×10^5 cells per well) in regular culture medium supplemented with 5% charcoal-stripped FCS instead of 10% normal FCS. After 24 h, cells were treated with various tin compounds for 48 h. At the end of each treatment, cells were washed three times with PBS. Aromatase activity then was determined by tritium release assay. This method measures production of ^3H_2O, which forms as a result of aromatization of the substrate [1β-^{3}H]androst-4-ene-3,17-dione (New England Nuclear, Boston, MA). Serum-free medium containing [1β-^{3}H]androst-4-ene-3,17-dione solution (54 nM) was prepared, and 0.5 ml of this solution was added to each well. In addition, wells containing media alone were tested to provide control values for aromatase activity. After incubation for 1 h, each plate was placed on ice, and 200 μl of culture medium was withdrawn from each well. The medium was extracted with 500 μl chloroform, vortexed, and then centrifuged for 1 min at 9000 × *g*. A 100-μl aliquot of the aqueous phase was mixed with 100 μl of a 5% wt/vol charcoal 0.5% wt/vol dextran T-70 suspension, vortexed, and then incubated for 10 min. After centrifugation of the solution for 5 min at 9000 × *g*, a 150-μl aliquot was removed to measure the level of radioactivity by liquid scintillation.

Quantitative RT-PCR

Jar cells were seeded in 100-mm tissue culture plates (1×10^6 cells) and treated with various compounds in regular culture medium supplemented with 5% charcoal-stripped FCS instead of 10% normal FCS, after which total RNA was extracted from them using TRIzol reagent (Invitrogen). mRNA expression of hCGβ and aromatase in Jar cells was determined by quantitative RT-PCR, as previously described (27). Total RNA (5 μg) extracted from Jar cells was reverse transcribed using SuperScript II reagent (Invitrogen) and oligo-(dT) as primer. The reaction was performed by incubation for 1 h at 42 C. After termination of cDNA synthesis, reaction mixtures were diluted with 4 volumes of Tris-EDTA. Aliquots (2 μl) of diluted reverse transcribed products were amplified in a reaction mixture containing 2× buffer from the Quanti-Tect SYBR Green PCR kit (QIAGEN, Valencia, CA) and 0.5 μM of each primer by using LightCycler (Roche Diagnostics, Mannheim, Germany). After preincubation at 95 C for 15 min, PCR was performed with 35–40 cycles of denaturation at 95 C for 15 sec, annealing at 65 C for 30 sec, and elongation at 72 C for 10 sec. Primers used were as follows: human aromatase, 5′-CCGGCCTTGTTCGTATGGTCA-3′ and 5′-CAACACGTCCACATAGCCCGA-3′; hCGβ, 5′-CCGTGTGCATCACCGTCAACA-3′ and 5′-GTTGCACACCACCTGAGGCAG-3′; and human β-actin, 5′-CTACGAGCTGCCTGACGGC-3′ and 5′-GCCACAGGACTCCATGCCC-3′.

Plasmid Construction

Human RXRα and RARβ cDNAs were amplified by RT-PCR using total RNA from JEG-3 cells. The amplified RXRα fragment was cloned into pSVSPORT1 (Invitrogen), whereas the RARβ fragment was cloned into a simian virus 40 promotor-containing expression vector. The resulting RXRα and RARβ expression vectors were termed pSVhRXRα and pSV40hRARβ, respectively. A 2.4-kb promoter I.1 sequence of the human aromatase gene (−2295 to +107 bp) was PCR amplified from JEG-3 genomic DNA. *Kpn*I and *Sma*I sites were introduced into the 5′- and 3′-termini, respectively, of the amplified fragment, which then was subcloned into the *Kpn*I–*Sma*I site of PGVB2 (Nippon Gene, Tokyo, Japan); the resulting reporter construct was termed PGVArom.

To construct a reporter plasmid containing an RXRE and RAR response element, response elements were cloned into the *Sma*I site of pTAL-Luc (CLONTECH Laboratories, Inc., Palo Alto, CA); response elements with the *underlined* consensus hexanucleotide sequence were as follows: DR1 × 2 (5′-AGGTCA a AGGTCA a AGGTCA a AGGTCA-3′); DR2 × 2 (5′- aa AGGTCA aa AGGTCA ccatcccgggaaa AGGTCA aa AGGTCA cc-3′); DR5 × 2 (5′-aa AGGTCA ccgaa AGGTCA ccatcccgggaaa AGGTCA ccgaa AGGTCA cc-3′); the resulting reporter constructs were termed pTALDR1, pTALDR2, and pTALDR5, respectively. The LBDs of hRXRα (codons 201–693), hRXRβ (codons 275–534), and hRXRγ (codons 172–455) were amplified by RT-PCR using mRNA from human liver and kidney and subcloned into pGEX-4T (Amersham Biosciences, Piscataway, NJ). These constructs were used for generation of glutathione *S*-transferase (GST)-hRXR fusion proteins. For chimeric receptor assay, the LBD of hRXRα was fused to the C-terminal end of GAL4-DNA binding domain (amino acids 1–147) in the pBK-CMV expression vector (Stratagene, La Jolla, CA) to yield pBK-CMV-GAL4-hRXRα. All sequences synthesized by PCR were confirmed by DNA sequencing. The plasmid p4×UAS-tk-luc, a LUC reporter construct containing four copies of the GAL4 binding site [upstream activating sequence (UAS) of GAL1] followed by a thymidine kinase promoter, was a kind gift from Dr. Y. Kamei (National Institute of Health and Nutrition, Japan).

Transient Transfection Assay

Transfection was performed with Lipofectamine regent (Invitrogen) in accordance with the manufacturer's instructions. JEG-3 cells (3×10^4 cells) were seeded in 24-well plates 24 h before transfection with the optimal dose of each DNA construct. At 18 h after transfection, various compounds were added to the transfected cells, which were then cultured in regular culture medium supplemented with 1% charcoal-stripped FCS instead of 10% normal FCS. The cells were harvested 30 h later, and extracts were prepared and assayed for LUC activity by using the dual-LUC reporter assay system (Promega Corp., Madison, WI) in accordance with the manufacturer's instructions. To normalize LUC activity for transfection and harvesting efficiency, the *Renilla* LUC control reporter construct pRL-TK (Promega) was cotransfected as an internal standard in all reporter experiments. The results are expressed as the average relative LUC activity of at least quadruplicate samples.

Ligand Binding Assay

The GST-RXR fusions were expressed in *Escherichia coli* DH5α cells and purified according to the manufacturer's (Amersham Biosciences) instructions. The purified proteins (30 μg/ml) were incubated with increasing concentrations of either [^{3}H]9cRA (1.63 tBq/mmol, Amersham Biosciences) or [^{14}C]TPTOH (2.04 gBq/mmol, Amersham Biosciences) with or without a 100-fold molar excess of each unlabeled compound. After incubation at 4 C for 1 h, specific binding was

determined by hydroxyapatite binding assay as described elsewhere (68). Binding in the presence of a 100-fold molar excess of unlabeled ligand was defined as nonspecific binding; specific binding was defined as total binding minus nonspecific binding. Similarly, tin compounds were used to compete for [^{3}H]9cRA and [^{14}C]TPTOH in this assay to determine the binding preferences of RXRs.

Statistics

Data were analyzed by the two-tailed unpaired Student's *t* test by using SPSS software (SPSS, Inc., Chicago, IL). Control and treatment group data were always obtained from equal numbers of replicate experiments. Values with $P < 0.05$ were considered statistically significant.

Acknowledgments

We thank Dr. Y. Kamei (National Institute of Health and Nutrition, Tokyo, Japan) for providing the plasmid p4xUAS-tk-luc and Teikoku Hormone Manufacturing (Tokyo, Japan) for the standardized hCG for ELISA.

Received October 7, 2004. Accepted June 1, 2005.

Address all correspondence and requests for reprints to: Dr. Tsuyoshi Nakanishi, Department of Toxicology, Graduate School of Pharmaceutical Sciences, Osaka University, 1–6, Yamadaoka Suita, Osaka 565-0871, Japan. E-mail: nakanishi@phs.osaka-u.ac.jp.

This work was supported in part by grants from a Grant in Aid for Scientific Research (nos. 13470499 and 15201012) from the Ministry of Education, Science, Sports, and Culture of Japan; Industrial Technology Research Grant Program in 2001 from New Energy and Industrial Technology Development Organization of Japan; Health and Labor Sciences Research Grants (Research on Advanced Medical Technology) from the Ministry of Health, Labor and Welfare of Japan; and The Long-Range Research Initiative, Japan.

REFERENCES

1. Chambon P 1996 A decade of molecular biology of retinoic acid receptors. FASEB J 10:940–954
2. Aranda A, Pascual A 2001 Nuclear hormone receptors and gene expression. Physiol Rev 81:1269–1304
3. Giguere V 1994 Retinoic acid receptors and cellular retinoid binding proteins: complex interplay in retinoid signaling. Endocr Rev 15:61–79
4. Sapin V, Ward SJ, Bronner S, Chambon P, Dolle P 1997 Differential expression of transcripts encoding retinoid binding proteins and retinoic acid receptors during placentation of the mouse. Dev Dyn 208: 199–210
5. Sapin V, Dolle P, Hindelang C, Kastner P, Chambon P 1997 Defects of the chorioallantoic placenta in mouse RXRα null fetuses. Dev Biol 191:29–41
6. Wendling O, Chambon P, Mark M 1999 Retinoid X receptors are essential for early mouse development and placentogenesis. Proc Natl Acad Sci USA 96: 547–551
7. Mascrez B, Mark M, Krezel W, Dupe V, LeMeur M, Ghyselinck NB, Chambon P 2001 Differential contributions of AF-1 and AF-2 activities to the developmental functions of RXRα. Development 128:2049–2062
8. Noback CR, Takahashi YI 1978 Micromorphology of the placenta of rats reared on marginal vitamin-A-deficient diet. Acta Anat (Basel) 102:195–202
9. Guibourdenche J, Alsat E, Soncin F, Rochette-Egly C, Evain-Brion D 1998 Retinoid receptors expression in human term placenta: involvement of RXRα in retinoid induced-hCG secretion. J Clin Endocrinol Metab 83: 1384–1387
10. Guibourdenche J, Roulier S, Rochette-Egly C, Evain-Brion D 1998 High retinoid X receptor expression in JEG-3 choriocarcinoma cells: involvement in cell function modulation by retinoids. J Cell Physiol 176: 595–601
11. Roulier S, Rochette-Egly C, Rebut-Bonneton C, Porquet D, Evain-Brion D 1994 Nuclear retinoic acid receptor characterization in cultured human trophoblast cells: effect of retinoic acid on epidermal growth factor receptor expression. Mol Cell Endocrinol 105:165–173
12. Matsuo H, Strauss III JF 1994 Peroxisome proliferators and retinoids affect JEG-3 choriocarcinoma cell function. Endocrinology 135:1135–1145
13. Sun T, Zhao Y, Mangelsdorf DJ, Simpson ER 1998 Characterization of a region upstream of exon I. 1 of the human CYP19 (aromatase) gene that mediates regulation by retinoids in human choriocarcinoma cells. Endocrinology 139:1684–1691
14. Tarrade A, Schoonjans K, Guibourdenche J, Bidart JM, Vidaud M, Auwerx J, Rochette-Egly C, Evain-Brion D 2001 PPARγ/RXRα heterodimers are involved in human CGβ synthesis and human trophoblast differentiation. Endocrinology 142:4504–4514
15. Zhu SJ, Li Y, Li H, Wang YL, Xiao ZJ, Vihko P, Piao YS 2002 Retinoic acids promote the action of aromatase and 17β-hydroxysteroid dehydrogenase type 1 on the biosynthesis of 17β-estradiol in placental cells. J Endocrinol 172:31–43
16. Simpson ER, Mahendroo MS, Means GD, Kilgore MW, Hinshelwood MM, Graham-Lorence S, Amarneh B, Ito Y, Fisher CR, Michael MD, Mendelson CR, Bulun SE 1994 Aromatase cytochrome P450, the enzyme responsible for estrogen biosynthesis. Endocr Rev 15: 342–355
17. Albrecht ED, Pepe GJ 1990 Placental steroid hormone biosynthesis in primate pregnancy. Endocr Rev 11: 124–150
18. Shozu M, Akasofu K, Harada T, Kubota Y 1991 A new cause of female pseudohermaphroditism: placental aromatase deficiency. J Clin Endocrinol Metab 72: 560–566
19. Yoshimi T, Strott CA, Marshall JR, Lipsett MB 1969 Corpus luteum function in early pregnancy. J Clin Endocrinol Metab 29:225–230
20. Huhtaniemi IT, Korenbrot CC, Jaffe RB 1977 hCG binding and stimulation of testosterone biosynthesis in the human fetal testis. J Clin Endocrinol Metab 44: 963–967
21. Boyer IJ 1989 Toxicity of dibutyltin, tributyltin and other organotin compounds to humans and to experimental animals. Toxicology 55:253–298
22. Fent K 1996 Ecotoxicology of organotin compounds. Crit Rev Toxicol 26:1–117
23. Horiguchi T, Shiraishi H, Shimizu M, Morita M 1997 Effects of triphenyltin chloride and five other organotin compounds on the development of imposex in the rock shell, *Thais clavigera.* Environ Pollut 95:85–91
24. Matthiessen P, Gibbs PE 1998 Critical appraisal of the evidence for tributyltin-mediated endocrine disruption in mollusks. Environ Toxicol Chem 17:37–43
25. Kannan K, Tanabe S, Iwata H, Tatsukawa R 1995 Butyltins in muscle and liver of fish collected from certain Asian and Oceanian countries. Environ Pollut 90:279–290
26. Kannan K, Tanabe S, Tatsukawa R 1995 Occurrence of butyltin residues in certain foodstuffs. Bull Environ Contam Toxicol 55:510–516

27. Nakanishi T, Kohroki J, Suzuki S, Ishizaki J, Hiromori Y, Takasuga S, Itoh N, Watanabe Y, Utoguchi N, Tanaka K 2002 Trialkyltin compounds enhance human CG secretion and aromatase activity in human placental choriocarcinoma cells. J Clin Endocrinol Metab 87:2830–2837
28. Chen CW, Hurd C, Vorojeikina DP, Arnold SF, Notides AC 1997 Transcriptional activation of the human estrogen receptor by DDT isomers and metabolites in yeast and MCF-7 cells. Biochem Pharmacol 53: 1161–1172
29. Korach KS, Sarver P, Chae K, McLachlan JA, McKinney JD 1988 Estrogen receptor-binding activity of polychlorinated hydroxybiphenyls: conformationally restricted structural probes. Mol Pharmacol 33: 120–126
30. Krishnan AV, Stathis P, Permuth SF, Tokes L, Feldman D 1993 Bisphenol-A: an estrogenic substance is released from polycarbonate flasks during autoclaving. Endocrinology 132:2279–2286
31. Kuiper GG, Lemmen JG, Carlsson B, Corton JC, Safe SH, van der Saag PT, van der Burg B, Gustafsson JA 1998 Interaction of estrogenic chemicals and phytoestrogens with estrogen receptor β. Endocrinology 139:4252–4263
32. Moore M, Mustain M, Daniel K, Chen I, Safe S, Zacharewski T, Gillesby B, Joyeux A, Balaguer P 1997 Antiestrogenic activity of hydroxylated polychlorinated biphenyl congeners identified in human serum. Toxicol Appl Pharmacol 142:160–168
33. Routledge EJ, Sumpter JP 1997 Structural features of alkylphenolic chemicals associated with estrogenic activity. J Biol Chem 272:3280–3288
34. White R, Jobling S, Hoare SA, Sumpter JP, Parker MG 1994 Environmentally persistent alkylphenolic compounds are estrogenic. Endocrinology 135:175–182
35. Kliewer SA, Umesono K, Noonan DJ, Heyman RA, Evans RM 1992 Convergence of 9-cis retinoic acid and peroxisome proliferator signalling pathways through heterodimer formation of their receptors. Nature 358: 771–774
36. Issemann I, Prince RA, Tugwood JD, Green S 1993 The peroxisome proliferator-activated receptor:retinoid X receptor heterodimer is activated by fatty acids and fibrate hypolipidaemic drugs. J Mol Endocrinol 11:37–47
37. Bardot O, Aldridge TC, Latruffe N, Green S 1993 PPAR-RXR heterodimer activates a peroxisome proliferator response element upstream of the bifunctional enzyme gene. Biochem Biophys Res Commun 192: 37–45
38. Westin S, Kurokawa R, Nolte RT, Wisely GB, McInerney EM, Rose DW, Milburn MV, Rosenfeld MG, Glass CK 1998 Interactions controlling the assembly of nuclear-receptor heterodimers and co-activators. Nature 395:199–202
39. Schulman IG, Shao G, Heyman RA 1998 Transactivation by retinoid X receptor-peroxisome proliferator-activated receptor γ (PPAR γ) heterodimers: intermolecular synergy requires only the PPAR γ hormone-dependent activation function. Mol Cell Biol 18:3483–3494
40. Laffitte BA, Kast HR, Nguyen CM, Zavacki AM, Moore DD, Edwards PA 2000 Identification of the DNA binding specificity and potential target genes for the farnesoid X-activated receptor. J Biol Chem 275: 10638–10647
41. Germain P, Iyer J, Zechel C, Gronemeyer H 2002 Co-regulator recruitment and the mechanism of retinoic acid receptor synergy. Nature 415:187–192
42. Allenby G, Bocquel MT, Saunders M, Kazmer S, Speck J, Rosenberger M, Lovey A, Kastner P, Grippo JF, Chambon P, Levin AA 1993 Retinoic acid receptors and retinoid X receptors: interactions with endogenous retinoic acids. Proc Natl Acad Sci USA 90:30–34
43. Sebastian S, Bulun SE 2001 A highly complex organization of the regulatory region of the human CYP19 (aromatase) gene revealed by the Human Genome Project. J Clin Endocrinol Metab 86:4600–4602
44. Bulun SE, Sebastian S, Takayama K, Suzuki T, Sasano H, Shozu M 2003 The human CYP19 (aromatase P450) gene: update on physiologic roles and genomic organization of promoters. J Steroid Biochem Mol Biol 86:219–224
45. Jameson JL, Hollenberg AN 1993 Regulation of chorionic gonadotropin gene expression. Endocr Rev 14: 203–221
46. Jameson JL, Lindell CM, Habener JF 1987 Gonadotropin and thyrotropin α- and β-subunit gene expression in normal and neoplastic tissues characterized using specific messenger ribonucleic acid hybridization probes. J Clin Endocrinol Metab 64:319–327
47. Saitoh M, Yanase T, Morinaga H, Tanabe M, Mu YM, Nishi Y, Nomura M, Okabe T, Goto K, Takayanagi R, Nawata H 2001 Tributyltin or triphenyltin inhibits aromatase activity in the human granulosa-like tumor cell line KGN. Biochem Biophys Res Commun 289: 198–204
48. Mu YM, Yanase T, Nishi Y, Takayanagi R, Goto K, Nawata H 2001 Combined treatment with specific ligands for PPARγ:RXR nuclear receptor system markedly inhibits the expression of cytochrome P450arom in human granulosa cancer cells. Mol Cell Endocrinol 181:239–248
49. Mu YM, Yanase T, Nishi Y, Waseda N, Oda T, Tanaka A, Takayanagi R, Nawata H 2000 Insulin sensitizer, troglitazone, directly inhibits aromatase activity in human ovarian granulosa cells. Biochem Biophys Res Commun 271:710–713
50. Thompson PD, Jurutka PW, Haussler CA, Whitfield GK, Haussler MR 1998 Heterodimeric DNA binding by the vitamin D receptor and retinoid X receptors is enhanced by 1,25-dihydroxyvitamin D3 and inhibited by 9-cis-retinoic acid. Evidence for allosteric receptor interactions. J Biol Chem 273:8483–8491
51. Forman BM, Umesono K, Chen J, Evans RM 1995 Unique response pathways are established by allosteric interactions among nuclear hormone receptors. Cell 81:541–550
52. Castillo AI, Sanchez-Martinez R, Moreno JL, Martinez-Iglesias OA, Palacios D, Aranda A 2004 A permissive retinoid X receptor/thyroid hormone receptor heterodimer allows stimulation of prolactin gene transcription by thyroid hormone and 9-cis-retinoic acid. Mol Cell Biol 24:502–513
53. Lala DS, Mukherjee R, Schulman IG, Koch SS, Dardashti LJ, Nadzan AM, Croston GE, Evans RM, Heyman RA, 1996 Activation of specific RXR heterodimers by an antagonist of RXR homodimers. Nature 383: 450–453
54. Kimmel EC, Fish RH, Casida JE 1976 Bioorganotin chemistry. Metabolism of organotin compounds in microsomal monooxygenase systems and in mammals. J Agric Food Chem 25:1–9
55. Ohhira S, Matsui H 2003 Metabolism of a tetraphenyltin compound in rats after a single oral dose. J Appl Toxicol 23:31–35
56. Ohhira S, Watanabe M, Matsui H 2003 Metabolism of tributyltin and triphenyltin by rat, hamster and human hepatic microsomes. Arch Toxicol 77:138–144
57. Unsworth B, Hennen S, Krishnakumaran A, Ting P, Hoffman N 1974 Teratogenic evaluation of terpenoid derivatives. Life Sci 15:1649–1655

58. de Urquiza AM, Liu S, Sjoberg M, Zetterstrom RH, Griffiths W, Sjovall J, Perlmann T 2000 Docosahexaenoic acid, a ligand for the retinoid X receptor in mouse brain. Science 290:2140–2144
59. Goldstein JT, Dobrzyn A, Clagett-Dame M, Pike JW, DeLuca HF 2003 Isolation and characterization of unsaturated fatty acids as natural ligands for the retinoid-X receptor. Arch Biochem Biophys 420:185–193
60. Harmon MA, Boehm MF, Heyman RA, Mangelsdorf DJ 1995 Activation of mammalian retinoid X receptors by the insect growth regulator methoprene. Proc Natl Acad Sci USA 92:6157–6160
61. Kitareewan S, Burka LT, Tomer KB, Parker CE, Deterding LJ, Stevens RD, Forman BM, Mais DE, Heyman RA, McMorris T, Weinberger C 1996 Phytol metabolites are circulating dietary factors that activate the nuclear receptor RXR. Mol Biol Cell 7:1153–1166
62. Lemotte PK, Keidel S, Apfel CM 1996 Phytanic acid is a retinoid X receptor ligand. Eur J Biochem 236: 328–333
63. Kagechika H 2002 Novel synthetic retinoids and separation of the pleiotropic retinoidal activities. Curr Med Chem 9:591–608
64. Egea PF, Mitschler A, Moras D 2002 Molecular recognition of agonist ligands by RXRs. Mol Endocrinol 16: 987–997
65. Benya TJ 1997 Bis(tributyltin) oxide toxicology. Drug Metab Rev 29:1189–1284
66. Watanabe H, Adachi R, Hirayama A, Kasahara T, Suzuki K 2003 Triphenyltin enhances the neutrophilic differentiation of promyelocytic HL-60 cells. Biochem Biophys Res Commun 306:26–31
67. Yamabe Y, Hoshino A, Imura N, Suzuki T, Himeno S 2000 Enhancement of androgen-dependent transcription and cell proliferation by tributyltin and triphenyltin in human prostate cancer cells. Toxicol Appl Pharmacol 169:177–184
68. Clagett-Dame M, Repa JJ 1997 Generating and characterizing retinoid receptors from *Escherichia coli* and insect cell expression systems. Methods Enzymol 282:13–24

Molecular Endocrinology **is published monthly by The Endocrine Society (http://www.endo-society.org), the foremost professional society serving the endocrine community.**

2742–2750 Nucleic Acids Research, 2005, Vol. 33, No. 8
doi:10.1093/nar/gki560

Chromatin assembly factor Asf1p-dependent occupancy of the SAS histone acetyltransferase complex at the silent mating-type locus *HMLα*

Shigehiro Osada*, Mitsumasa Kurita, Jun-ichi Nishikawa and Tsutomu Nishihara

Laboratory of Environmental Biochemistry, Graduate School of Pharmaceutical Sciences, Osaka University, 1-6 Yamada-Oka, Suita, Osaka 565-0871, Japan

Received January 28, 2005; Revised and Accepted April 20, 2005

ABSTRACT

Transcriptional repression of the silent mating-type loci *HMLα* and *HMR*a in *Saccharomyces cerevisiae* is regulated by chromatin structure. Sas2p is a catalytic subunit of the SAS histone acetyltransferase (HAT) complex. Although many HATs seem to relieve chromosomal repression to facilitate transcriptional activation, *sas* mutant phenotypes include loss of *SIR1*-dependent silencing of *HMLα*. To gain insight into the mechanism of the SAS complex mediated silencing at *HMLα*, we investigated the expression and chromatin structure of the α2 gene in the *HMLα* locus. We found that deletion of *SAS2* in combination with a null allele of *SIR1* changed the chromatin structure of the precisely positioned nucleosome, which includes the mRNA start site of the α2 gene and derepressed α2 transcription. The Sas2p HAT domain was required for this silencing. Furthermore, chromatin immunoprecipitation analysis revealed that the SAS complex was associated with the *HMLα* locus, and *ASF1* (which encodes chromatin assembly factor Asf1p), but not *SIR1* and *SIR2*, was necessary for this localization. These data suggest that the HAT activity and *ASF1*-dependent localization of the SAS complex are required for *SIR1*-dependent *HMLα* silencing.

INTRODUCTION

Silencing affects gene repression in a regional rather than promoter- or sequence-specific manner (1). The structure of the chromatin itself can affect gene expression, and changes in chromatin structure can result from the modification of histone tails as well as from the action of chromatin-remodeling complexes (2). A number of factors have been identified that contribute to transcriptional regulation by covalent modification of histones. In many cases, a relationship between histone acetylation and gene activation has been revealed by the identification of transcriptional co-activators, such as dedicated histone acetyltransferases (HATs) (3,4). Histone acetylation is reversed by histone deacetylases (HDACs), and many repression phenomena are regulated by HDACs (5). Moreover, HATs have been shown to contribute to repression and activation (4).

In *Saccharomyces cerevisiae*, silenced loci include the *HMLα* and *HMR***a** mating-type loci, the telomere regions and the ribosomal DNA repeats (2). A variety of proteins, including the silent information regulator (Sir) proteins, are required to silence the mating information genes at silent loci (6). One of the Sir proteins, Sir2p, possesses HDAC activity important for silencing (7,8). Disruption of the *SIR2*, *SIR3* or *SIR4* gene results in loss of silencing at *HM* loci, and a *SIR1*-disrupted strain is composed of mixed populations of silenced and unsilenced cells (9).

Something About Silencing (*SAS*) *2* was identified as an enhancer of *sir1* epigenetic *HMLα* silencing defects (10). Sas2p is a member of the MYST (MOZ, Ybf2/Sas3, Sas2 and TIP60) family of HATs and forms a complex, termed the SAS complex, with Sas4p and Sas5p (11–14). The SAS complex mainly acetylates histone H4 at lysine 16 (12–16). The role of *SAS2* in silencing is different for each silenced locus. At *HMLα*, deletion of *SAS2* has very little effect on silencing. However, deletion of *SAS2* combined with deletion of *SIR1* causes a severe silencing defect (10,17). Normal *HMR***a** silencing is unaffected by *SAS2* deletion, but *sas2* mutation suppresses the silencing defect caused by mutations in silencer elements of *HMR***a** (10,17). To determine the role of *SAS2* in rDNA silencing, a strain in which the *URA3* gene is integrated at the rDNA locus was used. The *sas2* deletion strain showed more effective *URA3* repression, indicating that the deletion of *SAS2* increased rDNA repression (12). In the case of telomeres, loss of *SAS2* causes hypoacetylation in adjacent sub-telomeric regions, leading to the recruitment of

*To whom correspondence should be addressed. Tel: +81 6 6879 8242; Fax: +81 6 6879 8244; Email: osada@phs.osaka-u.ac.jp

Sir3p to these regions and inactivation of gene expression (15,16). Therefore, *sas2* mutations reduce silencing of *HMLα* (when combined with deletion of *SIR1*) but improve silencing at *HMR***a** when accompanied by a weakened silencer element, hypoacetylated sub-telomeric regions, or the rDNA locus. To understand the differing roles of Sas2p, it is important to investigate the biochemical mechanisms by which these factors regulate gene silencing in each silent locus.

We previously showed that the chromatin assembly factor Asf1p interacts with the SAS complex, and *ASF1* and *SAS2* genetically function in the same pathway to repress the *HMLα* locus (11). In the present study, we show that *SAS2* is essential for the organization of the chromatin structure at *HMLα* in a *sir1* mutant and that *ASF1* is required for the recruitment of the SAS complex to the *HMLα* locus.

MATERIALS AND METHODS

Yeast strains, plasmids and manipulations

The strains used in this study are listed in Table 1 and were either published previously or were created for this study by using standard yeast manipulations (18,19). Expression plasmids of wild-type and mutant alleles of *SAS2* and *ASF1* were described previously (11). Mating assays were performed as described previously (11,20).

Table 1. Yeast strains used in this study

Strain[a]	Genotype	Source
W303-1a	MATa *ade2-1 his3-11, 15 leu2-3, 112 trp1-1 ura3-1 can1-100*	J. Workman
W303-1b	MATα *ade2-1 his3-11, 15 leu2-3, 112 trp1-1 ura3-1 can1-100*	J. Workman
YJW228	a *SAS4-13Myc:kanMX6*	J. Workman
YJW229	a *SAS5-13Myc:kanMX6*	J. Workman
YJW252	a *sir1Δ::LEU2*	D. Rivier
YJW253	a *sas2Δ::TRP1*	D. Rivier
YJW257	a *sir4Δ::URA3 lys2Δ::hisG*	D. Rivier
YJW258	a *sas2Δ::TRP1 sir1Δ::LEU2*	D. Rivier
YJW265	a *SAS2-13Myc:HIS3MX6*	J. Workman
YJW269	a *SAS2-13Myc:HIS3MX6 sas4Δ::kan*	J. Workman
YJW270	a *SAS2-13Myc:kanMX6 sas5Δ::HIS3*	J. Workman
YJW271	a *SAS2-13Myc:TRP sas4Δ::kan sas5Δ::HIS3*	J. Workman
YJW433	a *asf1Δ::HIS3MX6*	J. Workman
YJW435	a *asf1Δ::HIS3 sir1Δ::LEU2*	J. Workman
YJW436	a *asf1Δ::HIS3 sas2Δ::TRP1*	J. Workman
YS480	a *sir3Δ::HIS3MX6*	
YSM64	a *sir2Δ::HIS3MX6*	
YSM85	a *SAS2-13Myc:kanMX6 sir1Δ::HIS3MX6*	
YSM87	a *SAS2-13Myc:kanMX6 asf1Δ::HIS3MX6*	
YSM90	a *SAS2-13Myc:kanMX6 sir2Δ::HIS3MX6*	
YSM104	a *SAS2-13Myc:kanMX6 asf1Δ::HIS3MX6 sir1Δ::TRP*	
YSM112	W303-1a [pRS416/CEN/URA3 (pS14)]	
YSM113	YJW265 [pRS416/CEN/URA3 (pS14)]	
YSM114	YSM87 [pRS416/CEN/URA 3(pS14)]	
YSM115	YSM87 [Ycp50/CEN/URA3/ASF1 (pLS27)]	
YSM116	YSM104 [pRS416/CEN/URA3 (pS14)]	
YSM117	YSM104 [Ycp50/CEN/URA3/ASF1 (pLS27)]	
YSM118	W303-1a [pRS416/CEN/URA3 (pS15)]	
YSM119	W303-1b [pRS416/CEN/URA3 (pS15)]	
YSM120	YJW252 [pRS416/CEN/URA3 (pS15)]	
YSM121	YJW258 [pRS416/CEN/URA3 (pS15)]	
YSM122	YJW258 [pRS416/CEN/URA3/ PSAS2-SAS2 (pS126)]	
YSM123	YJW258 [pRS416/CEN/URA3/ PSAS2-SAS2-M1 (pS136)]	
YJW251[b]	α *his4*	D. Rivier

[a]Strains, except YJW251, are isogenic with W303-1a or W303-1b.
[b]YJW251 is a lawn strain for mating assays.

RNA blots

A 40 μg aliquot of total RNA prepared from logarithmically growing cells was separated on 1.0% agarose–formaldehyde gels and transferred to Hybond-N+ membranes (Amersham Biosciences, Piscataway, NJ). Specific messages were detected using randomly labeled α2 and *SCR1* probes.

High-resolution micrococcal nuclease mapping

Preparation of nuclei was carried out as described previously (21,22). Briefly, nuclei were isolated from yeast cells, which were grown to mid-log phase (OD_{600} = 1). The nuclear pellet from a 1 liter culture was resuspended in 2.4 ml digestion buffer (10 mM HEPES, pH 7.5, 0.5 mM $MgCl_2$ and 0.05 mM $CaCl_2$). The suspension was divided into 400 μl portions, each of which was digested at 37°C for 10 min by using increasing concentrations (0–16 U/ml) of micrococcal nuclease (MNase; Amersham Biosciences). The reaction was terminated by adding EDTA, and the DNA was purified after treatment with RNase, proteinase K digestion and phenol–chloroform extraction. The purified DNA was resuspended in 0.1× TE (1 mM Tris–HCl, pH 8.0, 0.1 mM EDTA). MNase cleavage sites were detected by multiple rounds of *Taq* DNA polymerase-based primer extension. The primer (5′-TATGTCTAGTATG-CTGGATTTAAACTCAT-3′) was end-labeled by T4 polynucleotide kinase. The cycling program was 94°C for 1 min, 53°C for 2 min and 72°C for 2 min for 35 cycles, and was followed by a 10 min chase at 72°C. The products were electrophoresed on a 6% polyacrylamide–8 M urea gel. The gel was dried and used to expose X-ray film. Relative MNase sensitivity was expressed graphically after scanning the autoradiogram and analyzing the scan by the NIH Image program (version 1.62).

Chromatin immunoprecipitation assay

The chromatin immunoprecipitation (ChIP) assay was performed essentially as described previously (23,24). A 50 ml culture of yeast (OD_{600} = 1) was treated with formaldehyde (final concentration of 1%) for 30 min at 20°C, and 2.5 ml of 2 M glycine was added to stop the cross-linking reaction. Cells were harvested and disrupted by vortexing in the presence of glass beads, and the lysate was sonicated to generate DNA fragments that ranged in size from 200 to 800 bp. To immunoprecipitate Myc-tagged proteins and Sir2p, we incubated anti-Myc antibody (9E10, Roche, Indianapolis, IN) and anti-Sir2p antibody (Santa Cruz Biotech., Santa Cruz, CA), respectively, with the extract overnight at 4°C, and the extract–antibody mixture then was incubated for an additional 3–4 h with protein G Sepharose beads (Amersham Biosciences). In some experiments, Myc-blocking peptide (Roche, final concentration 313 μg/ml) was added. Immunoprecipitates were washed with 1 ml each of lysis buffer (50 mM HEPES, pH 7.5, 140 mM NaCl, 1 mM EDTA, 1% Triton X-100, 0.1% sodium deoxycholate, 1 mM phenylmethylsulfonyl fluoride, 1 μg/ml leupeptin and 1 μg/ml pepstatin A), lysis buffer supplemented with 250 mM NaCl (for Myc-tagged Sas proteins) or 500 mM

NaCl (for Sir2p), LiCl–detergent wash buffer (250 mM LiCl, 10 mM Tris–HCl, pH 8.0, 1 mM EDTA, 0.5% NP-40 and 0.5% sodium deoxycholate) and TE. DNA was eluted with elution buffer (50 mM Tris–HCl, pH 8.0, 10 mM EDTA and 1% SDS). After reversal of the formaldehyde-induced cross-links, 1/5000 of input DNA and 1/45 of each immunoprecipitated DNA were used as templates for amplification by PCR. The sequences of primers for PCR were as follows: for the *HMLα* region, 5′-ATGCTCAGCTAGACGTTTTTCTTTC-3′ and 5′-TATGTCTAGTATGCTGGATTTAAACTCAT-3′; for the *ACT1* promoter region, 5′-CTTTTTCTTCCACGTCCTCTT-GC-3′ and 5′-TGGGATGGTGCAAGCGC-3′; and for the sub-telomeric chromatin at 7.5 kb from the end of chromosome VI, 5′-TCATGGTCTTGACAACTTTATGCG-3′ and 5′-TATC-TGACGTGAAAGTTCAGCGC-3′. Amplification was performed in a 20 µl reaction volume. The number of PCR cycles yielding product within the linear range was determined by analysis of 2-fold serial dilutions of the starting materials, and PCR products were separated on a 6% polyacrylamide gel and were detected by autoradiography. For quantitative analysis, 0.025 µl of [^{32}P]dCTP (110 TBq/mmol; Amersham Biosciences) was added to the PCR. After electrophoresis, the gel was dried, and the radioactivity corresponding to a specific band was measured by a bioimage analyzer (model BAS 1800II, Fuji Film, Tokyo, Japan).

Determination of the molecular size of the SAS-containing complex

Whole-cell extracts were prepared as described previously (11,25). Approximately 0.4 mg of each whole-cell extract was loaded onto a 2.4 ml Superdex 200 PC 3.2/30 column (Amersham Biosciences) that had been equilibrated in buffer containing 50 mM Tris–HCl, pH 8.0, 500 mM NaCl, 10% glycerol, 0.1% Tween-20, 1 mM phenylmethylsulfonyl fluoride, 0.5 µg/ml leupeptin and 0.5 µg/ml pepstatin A. A 10 µl aliquot of each fraction was electrophoresed in an SDS–polyacrylamide gel, transferred to nitrocellulose membrane and detected with the ECL western blotting analysis detection system (Amersham Biosciences). Anti-Myc antibody (9E10, Roche) was used.

RESULTS

*HMLα*2 was derepressed in a *sas2 sir1*-deleted strain

The α2 protein, which is a repressor of transcription of **a**-specific genes, is encoded by *MATα* and an essential factor for the regulation of mating-type-specific genes in α cells (26). The silent α information is also stored at the *HMLα* locus in both **a** and α cells. Previous work showed that the deletion of either *SIR1* or *SAS2* results in a very slight reduction of mating activity in a *MAT***a** strain, as indicated by quantitative mating analysis. The combined deletion of *SIR1* and *SAS2* strain causes a much more severe mating defect than that of the wild-type strain or the single-deletion strains (10,11). To show that the double deletion of *SAS2* and *SIR1* directly affects silencing at *HMLα*, we performed northern blotting analysis to detect the level of α2 mRNA in wild-type and deletion strains. α2 was transcribed not only in *MATα* cells but also in *sir4*Δ and *sas2*Δ*sir1*Δ *MAT***a** cells (Figure 1A).

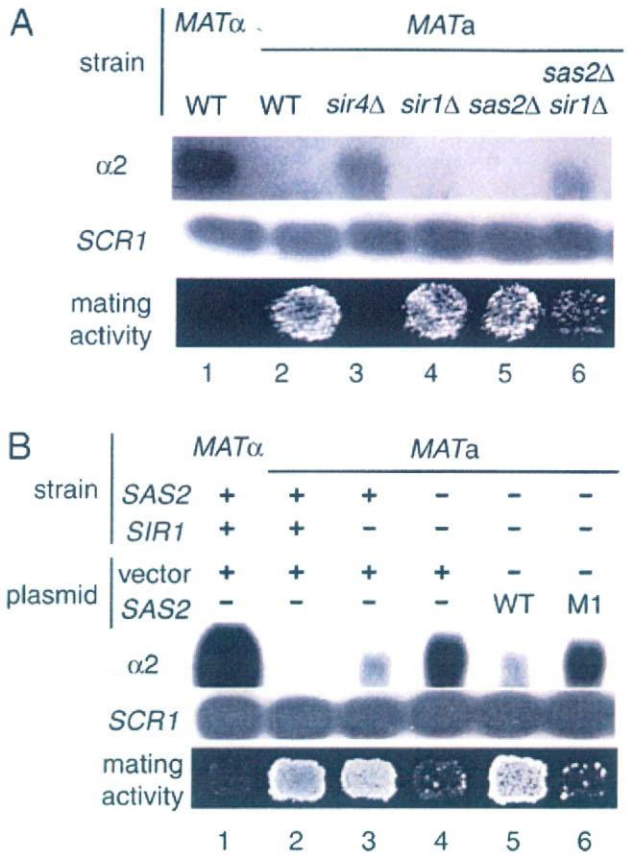

Figure 1. Deletion of *SAS2* and *SIR1* in a *MAT***a** strain leads to derepression of *HMLα*2 expression and a non-mating. (**A**) RNA from either wild-type (WT, W303-1b and W303-1a), *sir4*Δ (YJW257), *sir1*Δ (YJW252), *sas2*Δ (YJW253) or *sas2*Δ*sir1*Δ (YJW258) strains was hybridized by northern blotting to a probe specific for either the α2 or *SCR1* gene. RNA loading was standardized to *SCR1*. A qualitative mating assay was performed by patches, which were replica-plated to a lawn of *MATα* cells. WT and mutant strains are presented at the top of the panel. (**B**) A *sas2sir1* double-deletion strain was transformed with a plasmid carrying the WT or a mutant form of the *SAS2* gene (M1) under the control of its own promoter. Strains analyzed (ordered from left to right) were YSM119, YSM118, YSM120, YSM121, YSM122 and YSM123.

We previously showed that wild-type *SAS2*, but not *SAS2* with a mutation in the conserved HAT domain, could restore the mating activity of the *sas2*Δ*sir1*Δ strain. Furthermore, this mutation of amino acids 219–221 (GLG) to alanine residues (termed *SAS2*-M1) abolished the HAT activity of Sas2p but did not affect the formation of the SAS complex (11,13). To determine whether Sas2p HAT activity is required for the repression of α2 expression, wild-type and mutant *SAS2* alleles were transformed into the *sas2*Δ*sir1*Δ strain (Figure 1B). The mating activity and RNA level of α2 in the *sir1* mutant were the same as those of the *sas2 sir1* double-deletion strain carrying the wild-type *SAS2* expression plasmid (Figure 1B, compare lanes 3 and 5). *SAS2*-M1 failed to restore mating activity and α2 repression to the *sas2 sir1* double-mutant strain (Figure 1B, compare lanes 4 and 6). These results suggest that the Sas2p HAT activity is required for the repression of α2 expression from *HMLα* in a *sir1* mutant.

A strain with deletions of *SIR1* and *SAS2* shows loss of nucleosome organization at *HMLα*

The unique and highly organized chromatin structure of *HMLα* has been determined by high-resolution chromatin mapping analysis using MNase, which preferentially cuts the linker DNA between nucleosomes (27). Although a precisely positioned nucleosome (NUCα2) covers the transcription start site of the α2 gene at the *HMLα* locus, the promoter region of the α2 gene is nucleosome-free [(27); see also Figure 2A lanes 6–8 and Figure 2B]. We used MNase mapping to examine the effect of *sas2* mutations on the chromatin structure of *HMLα*. Deletion of *SIR4*, which is essential for *HMLα* silencing, resulted in increased nuclease sensitivity of one site, indicated by the arrow, compared with that of the wild type (Figure 2A, compare lanes 6–8 with lanes 10–12). Although we used downstream and reverse-strand primers in the attempt to visualize the positioning of NUCα2 clearly, we failed to obtain sufficient quantities of primer-extension products. For easy comparison of the MNase sensitivity, the lane treated with the highest concentration of MNase was selected for scanning (Figure 2A, lanes 8, 12, 16, 20 and 24). Relative MNase sensitivity is shown in Figure 2B after scanning and analyzing with the NIH Image software. The intensity of the induced sensitivity of the site highlighted in Figure 2A is the same in *sas2 sir1* double-deleted cells as in *SIR4*-deleted cells (compare lanes 10–12 with lanes 22–24) and stronger than that of wild-type or singly deleted strains (compare lanes 6–8, 14–16 and 18–20 with lanes 22–24). The MNase sensitivity of this site in different mutants correlates inversely with their mating activity and directly with the level of α2 mRNA (Figure 1A). These results suggest that *SAS2* is essential for the organization of the nucleosome precisely positioned over the transcriptional initiation site of the α2 in a *sir1*-mutant strain.

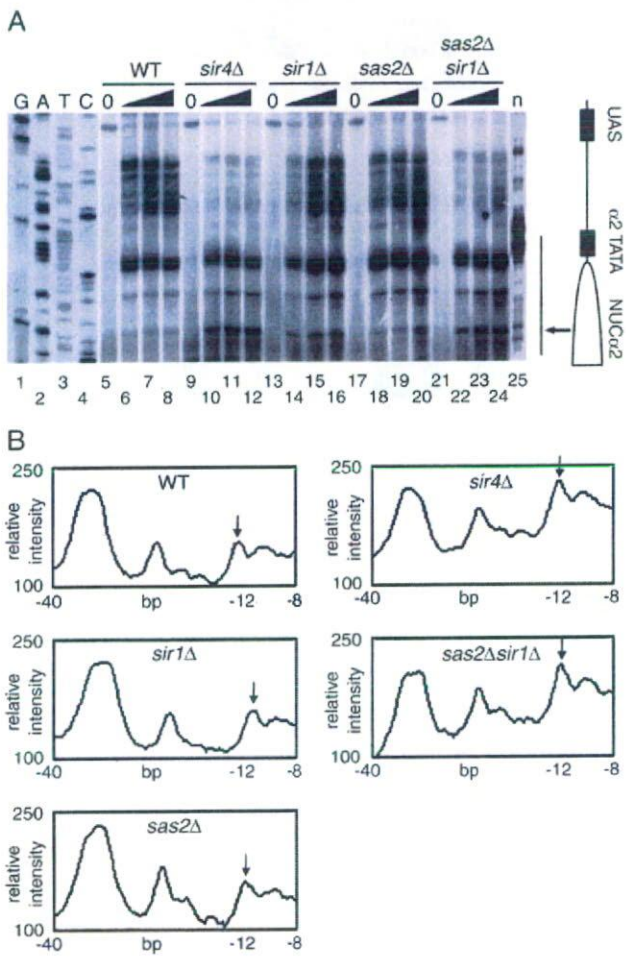

Figure 2. High-resolution MNase mapping of the promoter region of the α2 gene at the *HMLα* locus. (**A**) The chromatin structure of the Crick strand was mapped by primer-extension analysis of MNase-digested sites with the primer located at the coding region of the α2 gene. Strains used were as in Figure 1A. Extensions of undigested (0) and dose-dependent-digested chromatin are indicated. The 'n' lane shows the naked DNA digested with MNase (lane 25). The G, A, T and C columns indicate dideoxynucleotide-terminated sequencing reactions (lanes 1–4). The ellipse corresponds to the inferred position of the nucleosome, and boxes show the positions of the TATA-box and UAS regions. Arrow indicates sites in the α2 gene whose nuclease-sensitivity was increased in mutants relative to WT. The vertical bar indicates the region used for scanning to express the relative intensity in Figure 2B. (**B**) The relative MNase sensitivity expressed graphically after scanning and analyzing the autoradiogram in (**A**) by using NIH Image 1.62 software. Increased levels of nuclease-sensitive sites of the α2 gene in mutants (*sir4Δ* and *sas2Δsir1Δ*) relative to WT are indicated by arrows. The position from the transcription start site is shown at the bottom of each panel.

Interestingly, the nuclease sensitivity of the region between the UAS and TATA-box regions was decreased in *sas2Δsir1Δ* and *sir4Δ* strains. This region is generally less nuclease sensitive at *MATα* than at *HMLα* (27), and it is thought that in α2-positive cells, the protection of this region in chromatin from the nuclease might result from an association of transcription factors, including Rap1p, which bind to UAS (27). Overall, chromatin in this region is less accessible to nuclease in *sas2Δsir1Δ* strain than in wild-type strains.

The SAS complex associates with the *HMLα* locus

Genetic experiments revealed that combining the null allele of *SIR1* with that of *SAS2*, *SAS4*, *SAS5* or *ASF1* results in the reduction of silencing at *HMLα* (11,17). Meijsing and Ehrenhofer-Murray (12) reported that Sas2p is physically present at the rDNA locus, but not *ACT1*. To determine whether Sas2p or the SAS complex is located at the *HMLα* locus, we performed ChIP analysis using strains expressing Sas2p–Myc. Immunoprecipitated DNA was amplified by PCR with a primer pair spanning the α1 and α2 promoter regions in the *HMLα* locus (Figure 3A). We used *ACT1*, a gene whose transcription is not regulated by *SAS2*, as a negative control, because the *ACT1* mRNA level in the *sas2* mutant was same as that in the wild-type strain (15). Two-fold serial dilutions of the input and the immunoprecipitated DNA were performed to verify that the amount of PCR product was dependent on the starting material. Input DNA also was used as a template to confirm that these regions were amplified equally by PCR. In a *SAS2–Myc* strain, Sas2p–Myc associated with the promoter regions of the α1 and α2 in the *HMLα* region relative to *ACT1* (Figure 3A). This association was completely competed by adding a Myc-blocking peptide (compare lanes 11 and 12 with lanes 13 and 14).

We previously purified a complex containing Sas2p and showed that Sas4p and Sas5p were components of this

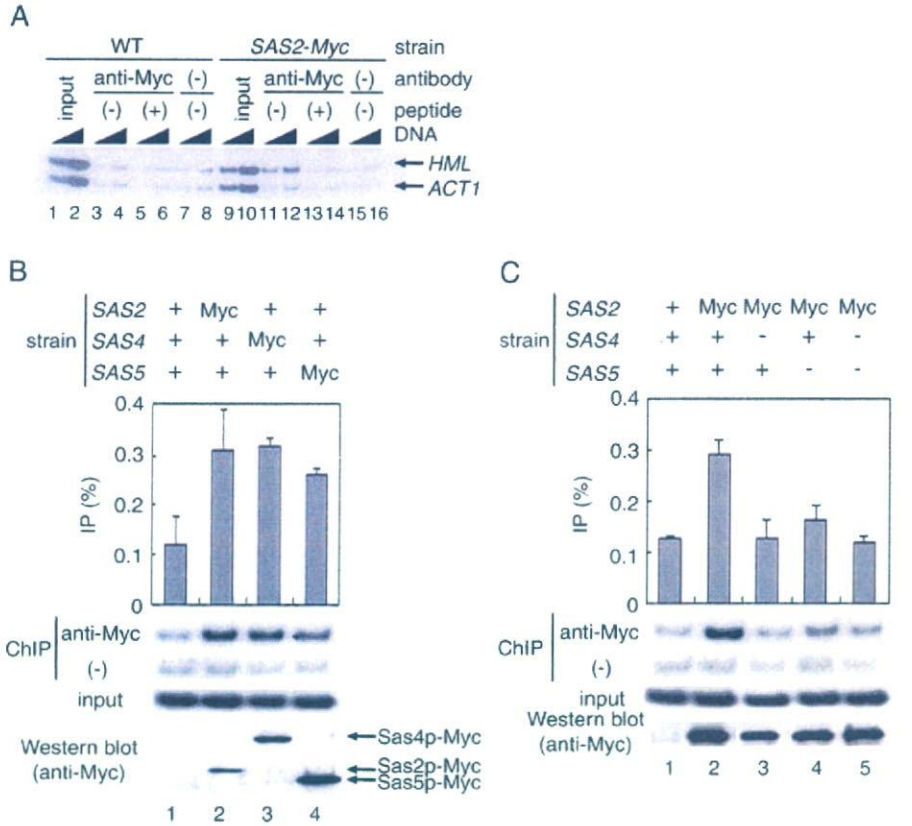

Figure 3. The SAS complex occupancy at the promoter in the *HMLα* locus. (**A**) Association of Sas2p with the *HMLα* region is detected by the ChIP assay. Sonicated chromatin was prepared from wild-type (WT) and Sas2p–Myc-expressing (YJW265) strains. Immunoprecipitation was carried out using monoclonal antibodies to the Myc tag (lanes 3–6 and 11–14), and normal IgG was used as a negative control (lanes 7, 8, 15 and 16). Myc-blocking peptide was added in some immunoprecipitation experiments (lanes 5, 6, 13 and 14). Input and immunoprecipitated DNA were amplified by PCR using primer pairs spanning the promoter region of α1 and α2 genes or *ACT1*. PCR products were resolved on a 6% polyacrylamide gel and visualized by autoradiography. (**B**) Localization of subunits of the SAS complex to the promoter of the α1 and α2 genes. Soluble chromatin was prepared from the strains that expressed the C-terminal Myc epitope-tagged Sas2p (YJW265), Sas4p (YJW228) or Sas5p (YJW229), and immunoprecipitated with or without anti-Myc antibody. Final DNA extractions were amplified with [^{32}P]dCTP. The PCR product was separated on the polyacrylamide gel and quantitated with a bioimage analyzer after drying the gel. ChIP efficiency is reported as a percentage of immunoprecipitated material (top panel). Data are presented as the mean ± SD from three independent experiments. Input DNA (input) was equally amplified by PCR in WT and Sas2p–Myc-expressing strains. Myc-tagged proteins were detected by western blotting (bottom panel). (**C**) *SAS4* or *SAS5* or both are required for the recruitment Sas2p to the *HMLα* locus. ChIP assay was performed with chromatin prepared from *sas4Δ* (YJW269), *sas5Δ* (YJW270) and *sas4Δsas5Δ* (YJW271) strains that expressed the C-terminal Myc epitope-tagged Sas2p. Results are shown as in Figure 3B.

complex, termed the SAS complex (11,13,14). We next asked whether Sas4p and Sas5p associate with the *HMLα* locus. ChIP analyses using *SAS4–Myc* and *SAS5–Myc* revealed that Sas4p–Myc and Sas5p–Myc were recruited together with Sas2p–Myc to the promoter regions of the α1 and α2 in the *HMLα* region (Figure 3B). This finding supports the possibility that these Sas proteins associate with chromatin as a complex. Accordingly, deletion of either *SAS4* or *SAS5* might disrupt the association of Sas2p with the *HMLα* locus.

To evaluate whether this disruption occurs, we performed ChIP using cells expressing Sas2p–Myc and deleted for *SAS4*, *SAS5* or both genes (Figure 3C). The amount of amplified PCR products from the three deletion strains was markedly lower than from the wild-type strain, although Sas2p–Myc was expressed efficiently in all of the *SAS2–Myc* strains. These results show that mutations in *SAS5* and especially *SAS4* inhibit the association of Sas2p–Myc with the promoter regions of the α1 and α2 in the *HMLα* region and that Sas2p–Myc was recruited to this region as a component of the SAS complex.

SIR1 and *SIR2* are not required for the recruitment of Sas2p to the promoters in the *HMLα* locus

Four Sir proteins localize to *HMLα* and *HMR***a** and are important for silencing. Sir1p binds to Orc1p, one of the silencer binding proteins, and helps to recruit Sir4p. Sir2p, Sir3p and Sir4p form a complex and spread in both directions from the silencers (1,28). A physical interaction between Sas and Sir proteins has not been reported, although all of them localize to the *HMLα* locus. To understand the role of the Sir proteins in the association of Sas2p with the *HMLα* locus, we first asked whether loss of Sir1p or Sir2p results in disruption of this association. To do this, Sas2p was tagged with Myc in *SIR1* or *SIR2* deletion strains. Western blot analysis revealed that Sas2p–Myc was expressed efficiently in both *SIR1* and *SIR2*